E.ON Energy Research Center

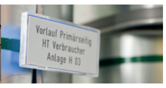

E.ON Energy Research Center Series

Energy Concept for the E.ON ERC Main Building

Johannes Fütterer, Ana Constantin

Volume 4, Issue 9

RWTHAACHEN UNIVERSITY

E.ON Energy Research Center

E.ON Energy Research Center Series

Energy Concept for the E.ON ERC Main Building

Johannes Fütterer, Ana Constantin

Volume 4, Issue 9

RWTH AACHEN UNIVERSITY

Contents

Executive summary

Within this project, we developed an energy concept for the new E.ON ERC main building. During the building's construction phase, we assisted the implementation of the energy concept and implemented an user-added monitoring system. Together with a virtual server infrastructure, different data bases, data processing algorithms, and interfaces, this system became the monitoring, control and interface system (MCIS) which transformed the building into a control research demonstration bench.

Enabled by the extensive data available, we were able to build and validate several simulation models for the building and for technical building equipment. These models were then used to set-up and run test scenarios for the development and improvement of control strategies for different parts of the energy concept.

Monitoring data analyses and simulation studies enabled extensive system assessment and optimization via gathered knowledge and system insights. From an control point of view, the project revealed serious defects which led to an high energy consumption. The optimization's result was a completely new control strategy, which we implemented in February 2014.

An online monitoring and data visualization system publishes daily, weekly, monthly and yearly building reports, integrated into the new E.ON ERC homepage. Further, a promotional display in the building's reception area informs about actual data points.

The implemented energy concept is able to fulfill all energy demands. Thermal comfort within the new building is more than acceptable.

The MCIS is in full operation and provides highly resolved monitoring data. Several up-following projects are enabled by the MCIS and are already taking advantage of the system.

With the help of the developed data processing framework it is possible to flexibly conduct assessments towards the energy conversion system, the energy distribution system, the energy usage and the thermal comfort.

1 Introduction

The project develops an energy concept for the new home for the five institutes of the E.ON Energy Research Center. The development challenge is to achieve highest standards of energy efficiency while reliably fulfilling the energy demands of the building. The multifunctional building integrates different areas for different use, thus, it is facing energy demand for climatization of offices, conference areas, laboratories, stuff facilities, such as student work spaces, as well as demand for process energy for the operation of test benches and experiments. The proposed concept consists of a combination of a geothermal field, a heat pump, a co-generation plant, and sorption-supported air handling units, together with efficient and demand-matching distribution strategies, such as displacement ventilation, active chilled beams, and façade ventilation units.

In order to gather data, verify and optimize the proposed concept an extensive beyond state-of-the-art monitoring-system is designed and integrated providing all possibilities for flexible data analysis, data visualization, and algorithm evaluation. Thermal, hydraulic, and component simulation models are developed. Data interfaces are set up to allow for model-predictive control, remote control, and external control strategy development and adjustments. The freely programmable building automation system together with simulations, monitoring, and data interfaces constructs a demonstration bench for all thinkable future control approaches, such as agent-based control, advanced rule-based control, and, as already mentioned above, model-predictive control.

Energy related building data is published via an internet presence where daily, weekly, and monthly reports are accessible. A promotional display shows live data within the building itself, a supervisory control and data acquisition system (SCADA) allowing for detailed live data and a MySQL event-based database offering historical data for each data point are accessible via the internet.

This report presents the new E.ON ERC main building itself, it introduces and explains the developed energy concept and describes the technical principles of the monitoring and interaction system. It presents the developed simulation models and shows simulation results. Results of energy-related data analysis and evaluations are presented for each layer and component of the energy concept. The paper concludes with topics that are still to address and a perspective of future research topics that are enabled by the installed infrastructure.

2 Building

The main building of the E.ON Energy Research Center (ERC) is located in the Campus Melaten of the RWTH Aachen University. The Campus Melaten is a new research park of the university, which is located in the western part of the city of Aachen, with a planned area of $473,000 \text{ m}^2$. Figure 2.1 shows the current layout of the campus, with the E.ON ERC building marked in red in the lower right corner.

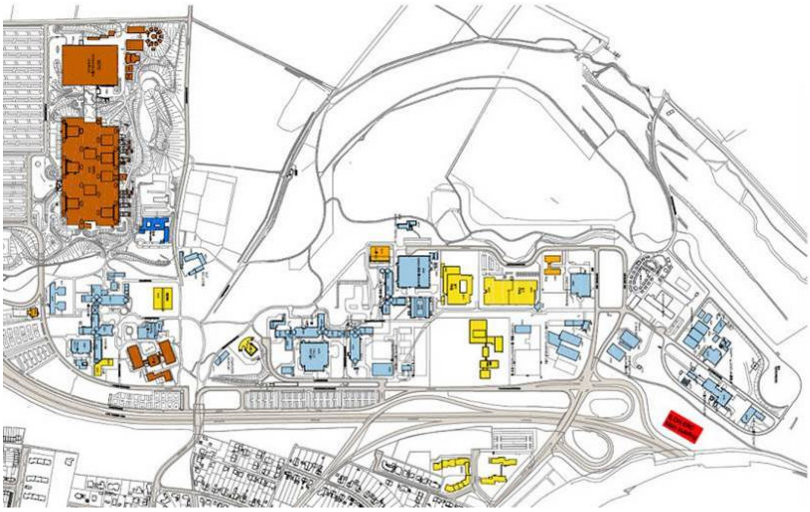

Figure 2.1: View of Campus Melaten with E.ON ERC main building marked in red in the lower right corner

The exact geographical location of the building is longitude: 50.7897°; latitude: 6.0512° in the northern hemisphere.

The construction of the building was started in August 2010 and finished in November 2011. It now houses the five institutes of the research center along with the administrative offices. The building is multi-functional, integrating the following different usable areas:

- Office rooms and staff facilities
- Seminar and conference rooms
- Laboratories
- Common area

Figures 2.2 and 2.3 present exterior and interior views of the building.

The building has a complex energy concept (see chapter 3). Because of time constraints the planning for the implementation of this concept was done concomitantly to the building process. Combined with the complexity of the system this lead to a suboptimal operation of the system once the building was completed. However because the building serves as an experimental object as well, a detailed monitoring system was installed after completion of the building, which helped to faster identify the suboptimal conditions. Usually such planning errors only reveal themselves in case of complete failure of the technical equipment, but in our case we were able to react sooner, because of the additional information provided by the measurements. The corrective actions needed to be taken after construction completion were further delayed by the general contractor going bankrupt. However as of May 2014 we are well underway in the implementation of these corrective measures (see chapter 6).

The ground floor area of the building is 58.43 m by 34.72 m leading to a useable area of $7,500\ m^2$ over four storeys: basement, ground floor and two upper floors. The roof of the building is used for a PV installation, a chiller and a roof top unit, which houses the two central air conditioning units. The building volume that needs to be conditioned is $23,500\ m^3$, which for an exterior area of the building envelope of $6,823\ m^2$ indicates a compact construction type [Maas et al., 2002].

Figure 2.2: Exterior view of E.ON ERC main building

Additionaly to the calculations made by the engineering firm, which was in charge of the construction, own static calculation for primary and net energy demand were done. To this purpose we used the Software EnerCalc [Lichtmeß, 2010]. The above mentioned performance indicators are calculated by splitting the building into zones according to their usage, and further more according to the conditioning concepts at place in those areas [DIN V 18599].

With U-values of 1.22 $\frac{W}{m^2 \cdot K}$ for windows and 0.19 $\frac{W}{m^2 \cdot K}$ for outer walls the building has a yearly pri-

Figure 2.3: Interior view of E.ON ERC main building

mary energy demand of 105.1 $\frac{kWh}{m^2 \cdot a}$ and a net energy demand of 68 $\frac{kWh}{m^2 \cdot a}$ which makes it compliant with the German Energy Saving Ordinance EnEV 2009 [EnE, 2009].

The layout of the upper floors, as seen in figure 2.4 is very open. Each office has at least one wall facing to the outside. In the middle there is a large corridor space and student work areas. The high atrium area created in this way reflects the main goal on the research center: to create an environment which encourages know-how transfer across different disciplines, as people from the different institutes are bound to cross each other paths when moving inside the building.

Figure 2.4: Layout second floor of the E.ON ERC main building

3 Energy Concept

3.1 System overview

Following the demand of the building, the energy has to be supplied on four different temperature levels: cooling energy at 6 °C for laboratory use, cooling energy at 17 °C and heating energy at 35 °C for thermal comfort needs as well as process heat at 80 °C for laboratory use and brine regeneration.

Figure 3.1 provides a visualization of the concept, consisting of three layers: energy conversion layer, energy distribution layer and energy demand layer. The energy conversion layer is based on geothermal energy and heat displacement in connection with a heat pump process. The heat pump is equipped with a variable-speed centrifugal compression with magnetic, oil-free bearings, providing a high efficiency in wide areas of partial load. The geothermal field consists of 40 boreholes, each 100 m deep. It serves as a source of environmental energy and as energy storage at the same time. A glycol cooler offers the possibility to dissipate energy directly to the environment. On the 80 °C temperature level, a gas-fired combined heat and power (CHP) unit provides process heat and electric power for heat pump operation. The power production is supported by photovoltaics installed on the building's roof. A condensing boiler system serves as a backup system for the heat pump and as a generation unit of process heat, exceeding the heat contributed by the gas-fired CHP unit. A sorption-supported air handling unit converts process heat directly into cooling energy for laboratories, CIP-Pools and conference spaces.

The heating and cooling base loads are distributed by concrete core activation in conference spaces, CIP-Pools and offices. The concrete core distribution system has high thermal capacity. Peak loads in heating and cooling are covered by façade ventilation units, equipped with four ways heat exchangers, able to cool and heat directly by air supply consisting either of fresh outside air or recirculation air, depending on thermal conditions, volatile organic compounds (VOC) and CO_2 levels inside the room. The façade ventilation units are able to recuperate heat or cold of exhaust air with high efficiency. Peak loads in conference spaces and CIP-Pools are covered by displacement ventilation with conditioned air provided by the sorption-supported air handling unit. Active chilled beams are controlling the thermal comfort at the laboratories.

The underlying principle of the concept is the use of geothermal energy and heat displacement. During winter, heat from the geothermal field and server rooms is integrated into the heat pump system. During summer, heat from the building, server rooms and laboratories is displaced to the

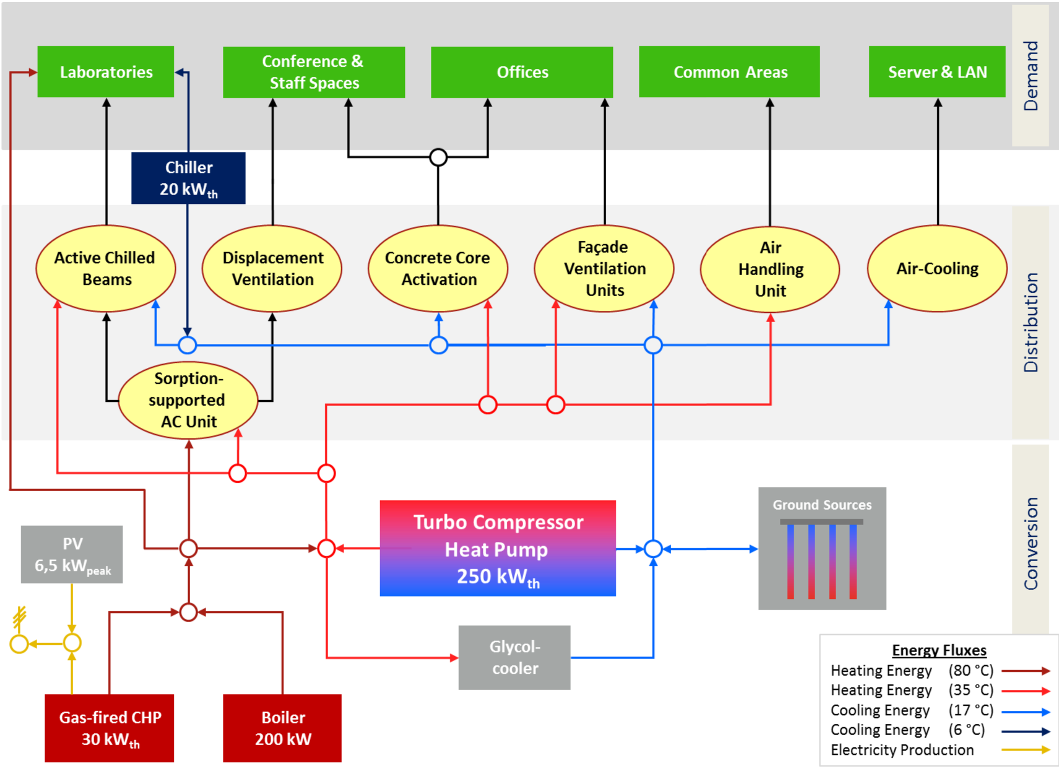

Figure 3.1: Schematic of the implemented energy concept

geothermal field or cooled down by the glycol cooling system. A passive cooling can be realized by the concrete core activation using cold water from the geothermal field.

Winter mode: The heat pump provides main heating energy. It is supplied by waste heat from server and LAN cooling as well as geothermal heat. The system keeps this operation principle during transition periods until the server and LAN waste heat is enough to supply the heat pump. From here on no more heat is extracted from the geothermal field.

Summer mode: During cooling periods the heat pump and the sorption-supported air handling unit supply the building with cooling energy. As long as the geothermal field is able to store further energy, the waste heat from the heat pump is lead into the field. Exceeding energy is dissipated by the glycol cooler. Simulations of the geothermal field show that brine supply temperatures are kept between 4 and 16 °C. In periods with moderate need for cooling, the heat pump reduces power or even stops working. Cooling will be provided by directly displacing heat from the building to the geothermal field.

Since test benches are operated and experimental work is performed in the building, there is a on-going but varying need for high-temperature heat and low-temperature cold throughout the year. The high-temperature circuit is supplied by the CHP and the condensing boiler system; the low-temperature circuit is supplied by the additional heat pump process, as it can be seen in Figure 3.1.

3.2 Control strategy

The building's technical planners tried to design an initial control and operation strategy during the building's planning phase, which was implemented during the building's construction. We learned that the planners obviously did not understand the complexity of the system, which resulted in an ongoing hand mode operation. We analyzed all systems of systems within the building as it is presented in chapter 6, especially chapter 6.1, and derived an all new control strategy. The control strategy has been developed basing on the results of mentioned analysis and basing on low exergetic approaches. It has been implemented during March 2014. The following chapter describes this new developed control strategy.

The proposed control strategy starts with an estimation of the heating and cooling loads and is then shifting between cooling and heating mode, resulting in operation of different energy conversion units as well as different energy sinks and sources.

3.2.1 Selecting the operation mode

According to the given system overview, a control strategy manages the interaction between each subsystem. The principal issue is an estimation of heating and cooling demand. This takes place in the "heat pump" subsystem. A 5000 l cooling and a 4000 l heating water storage are placed between the heat pump and the distribution system. Each storage tank contains four temperature sensors which allow for measuring the temperature in different layers. These temperatures are averaged to calculate a current energy potential of each storage:

$$E_{Potential} = \overline{T}_{Storage} \cdot V_{Storage} \cdot c_p \tag{3.1}$$

$E_{Potential}$ means the energy potential, $\overline{T}_{Storage}$ the mean storage temperature, $V_{Storage}$ the storage volume and c_p the isobar heat capacity.

The difference between the energy potential gradients of the two storages defines the operation mode:

$$\dot{E}_{Heating\ Storage} - \dot{E}_{Cooling\ Storage} >= 0: \quad winter\ mode \tag{3.2}$$

$$\dot{E}_{Heating\ Storage} - \dot{E}_{Cooling\ Storage} < 0: \quad summer\ mode \tag{3.3}$$

To avoid a distortion of the demand, the estimation is executed in a system state of no active energy provision by heat pump, glycol cooler or geothermal field. It means, that the storage systems cover the total heating and cooling demand. Therefore, the demand estimation is a periodic operation and starts after leaving either the winter or the summer mode and ends by entering one of the two operation modes.

3.2.2 Winter mode

In case of winter mode, the heat pump provides heating energy at a temperature level of 35 °C. It is controlled by a temperature hysteresis starting when the highest temperature sensor of the heating storage sinks below 30 °C and ends by reaching the 35 °C temperature at the top of the storage. Hydraulic and thermodynamic reflections leads to only one useful combination of all system components in winter mode. A schematic overview can be seen in figure 3.2.

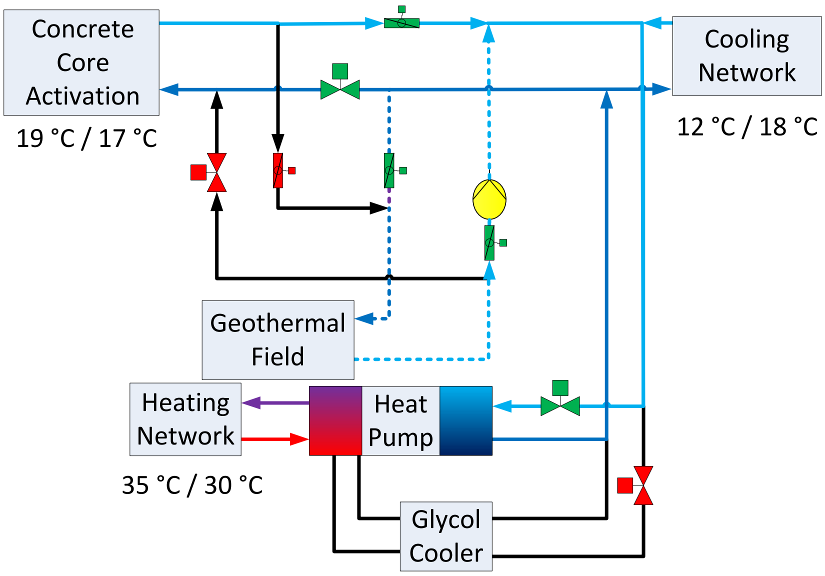

Figure 3.2: Schematic of the hydraulic system in winter mode

A red colored value means closed, respectively green opened. Black lines mean unused pipes, red (30 °C) and purple (35°C) mean heating water flow, brightly (17 °C - 18 °C) and dark blue (12 °C - 17 °C) cooling water flow. Dashed lines mark pipes, whose volume flows are controlled via valves, thus, having a 100% volume flow, no volume flow or a volume flow between 0% and 100%. The switching or controlled valves are colored yellow. The geothermal field starts supporting the cooling storage as soon as the cooling storage's mean temperature decreases below 12 °C. The possible support by the circulatory pump of the geothermal field is colored yellow and the additional flow direction is shown dashed. If the heat demand is not high enough to unload the heating storage in a period of ten minutes, the system ends the winter mode and starts a new periodic demand estimation for choosing the operation mode.

3.2.3 Summer mode

Hydraulic and thermodynamic thoughts lead to several combination possibilities of each of the subsystems in summer mode. Each combination depends on temperature limits and operation states of each of the subsystems. The possible system combinations get prioritized by energetic and economic aspects to deduce the course of action. Table 3.1 gives the list of possible combinations and their priority starting from one (highest priority) to seven (lowest priority).

Table 3.1: System combinations and priorities in summer mode

priority	heat pump	glycol cooler	geothermal field	heat demand
1	off	on	off	none
2	off	off	on	none
3	off	on	on	none
4	on	off	on	some
5	on	on	on	none
6	on	off	off	some
7	on	on	off	none

The control strategy allows to switch dynamically between these 7 operating combinations without leaving the summer mode. Several temperature limits guaranty a simple and stable system operation. If the heat pump is in use, it provides cooling energy at a temperature of 12 °C. The glycol cooler can be used to cool directly the cooling network at a temperature of 12 °C or to cool down the heating storage in case of heat pump use while no heat demand is needed.

The highest priority is the supply of all needed cooling demand by direct cooling via glycol cooler. Two conditions has to be fulfilled to run this mode: First, an outside temperature of less then 10 °C to guaranty a temperature gradient for the heat transfer from cooling network to the environment. Second, no or just little needed heat demand at the same time. This condition is fulfilled if the mean temperature of the heating water storage is higher then 31 °C. If one of theses two conditions is not fulfilled, the direct cooling via glycol cooler is not possible and another operation mode has to be chosen.

The next priority level is the supply of all needed cooling demand by the geothermal field. There are two conditions to start this mode similar to the previous one: First, an outlet temperature of the geothermal field of 12 °C or less to support both, the concrete core activation and the cooling network. Second, no or just little heat demand at the same time, implemented in a mean heating water storage temperature higher then 31 °C. The schematic of the hydraulic system for the first two operation modes is shown in 3.3. For alternative support either by glycol cooler or geothermal field, the switching valves are colored yellow and the addittonal flow directions are shown dashed.

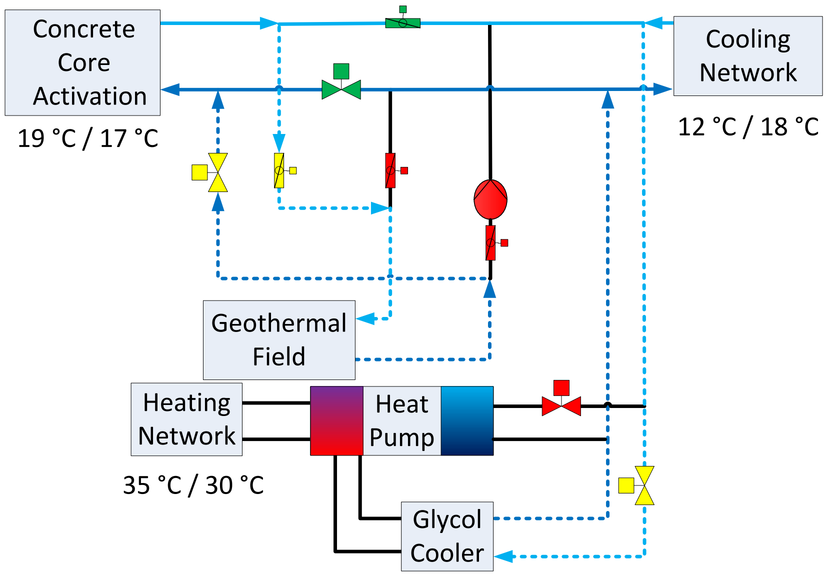

Figure 3.3: Schematic of the hydraulic system in priority level one and two in summer mode

If the outlet temperature of the geothermal field rises above 12 °C it can not be used to support the cooling network anymore. Therefore, the concrete core activation gets separated from the rest of the cooling network by closing a valve: The geothermal field supplies the concrete core activation while the glycol cooler (priority level three) or the heat pump (priority level four and five) supply the cooling network. For using the glycol cooler, the conditions are the same as in priority level one: outside temperature is less then 10 °C and the mean heating water storage temperature is higher then 31 °C. Otherwise, the heat pump will be used. The heat pump provides cooling energy at a temperature level of 12 °C. It is also controlled by a temperature hysteresis starting if the bottom temperature sensor of the cooling water storage rises above 12 °C and ends by reaching the 12 °C temperature at the top of the storage. In case of using the heat pump, two possibilities are given: Given high enough heating demand to hold the mean temperature of the heating water storage below 33 °C, no further action is needed (priority level four). Rises this temperature up to 33 °C, the glycol cooler cools the storage to 33 °C (priority level five).

A PID-controller regulates the linking valve of concrete core activation and the rest of the cooling network. The reference variable is the mixed inlet temperature of the concrete core activation and has a set point of 17 °C. That means if the outlet temperature of the geothermal field is below 17 °C, the valve is closed. Over 17 °C the valve is partial open to mix water of 12 °C from the cooling network to the outlet water of the geothermal field to reach the set point temperature of 17 °C. An overview of the hydraulic system for priority level three, four and five gives figure 3.4.

If the difference between outlet and inlet temperatures of the geothermal field is less then 0,5 K, the geothermal field is either exploited or the cooling demand is too low (in ratio to the pumping energy) and it will not be used for cooling anymore. It will be disabled and the linking valve be-

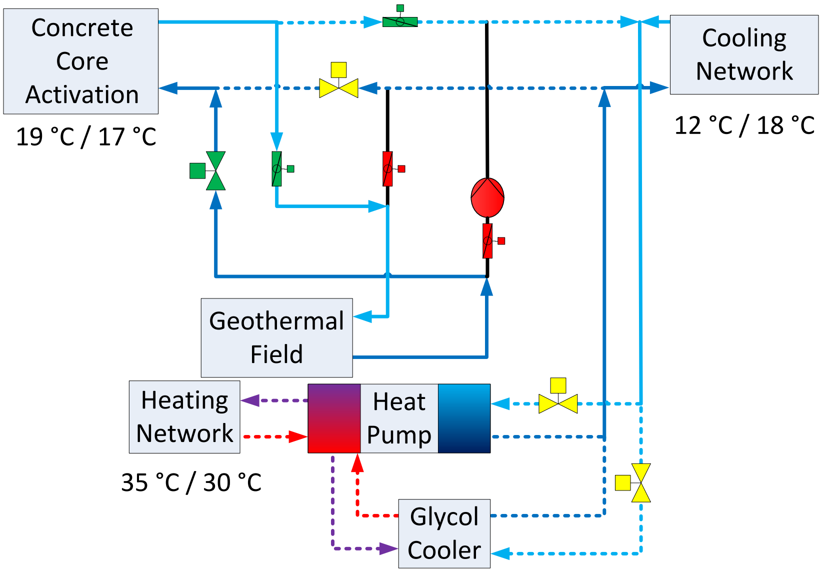

Figure 3.4: Schematic of the hydraulic system in priority level three, four and five in summer mode

tween concrete core activation and cooling network is entire open. Both has to be supported by glycol cooler (priority level one) or heat pump, either without (priority level six) or with additional re-cooling of the heating water storage (priority level seven). The decision is analog to the use with geothermal field operation. Figure 3.5 gives a schematic of the hydraulic system in priority level six and seven with alternatives shown in dashed lines.

If the heat pump, the geothermal field and the glycol cooler are disabled, the cooling and heating systems get supplied by the storages. If one of theses subsystems does not start after a given time of ten minutes, the system leaves the summer mode and starts a new cycle of estimating the heating and cooling demand.

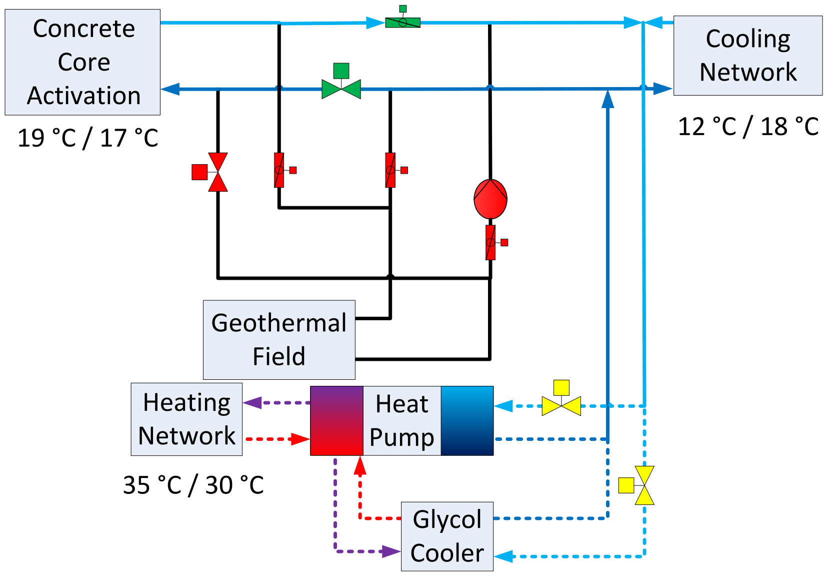

Figure 3.5: Schematic of the hydraulic system in priority level six and seven in summer mode

4 MCIS and control demonstration bench

The monitoring, control and interface system (MCIS) has been designed to achieve different goals. The goals of the MCIS are

- providing extensive data for evaluation, optimization, simulation validation.
- to provide prerequisites for automated energy and operation related evaluation and online publication,
- providing a system interface for flexible user interfaces, such as smart phone and web applications, and
- interfacing external intelligence for building control, such as model-predictive control, demand side management algorithms or control strategy development.

In order to achieve the goals, different kinds of data sources have to be integrated in the system. All physical input and output signals, network variables and control strategy parameters of the building automation system and all data points from different BACnet-devices are logged. To gather further relevant data an extensive monitoring system has been user-added.

Sensors and automation components, that have been installed during the construction process of the building, are not able to fulfill all prerequisites for an operational and energetic monitoring as it is described in the following chapter 4.1. Thus, it is necessary to place additional sensors within the building. These sensors are the so-called user-added monitoring sensors. The user-added sensors are mainly magnetic-inductive volume flow sensors, temperature, humidity and electrical power sensors.

An on-site weather station, delivering precise weather data and a detailed weather forecast are integrated. The system is equipped with a flexibly expandable wireless auto-routing sensor network. It is possible to store results of additional temporary measurements within the system. The MCIS provides interfaces for data analysis, remote control and external control algorithms.

A schematic of the functional principle can be found in figure 4.1. Data sources and sinks are directly connected to C#-services (C# is a computer programming language) or connected to an OPC-server (OPC is an abbreviation of object linking and embedding for process control). C#-services access the OPC-server, the weather forecast and a wireless sensor system. They store the data within two MySQL-databases, for weather data and all other historic data. The C#-services provide an interface for storing data of temporary measurements. External intelligence and user interfaces can communicate to the building via a TCP-interface, which makes it far more easy to connect with; compared to a direct OPC connection. The weather station, the building automation system, larger units of the technical building equipment and the user-added monitoring system are integrated within a BACnet/IP network.

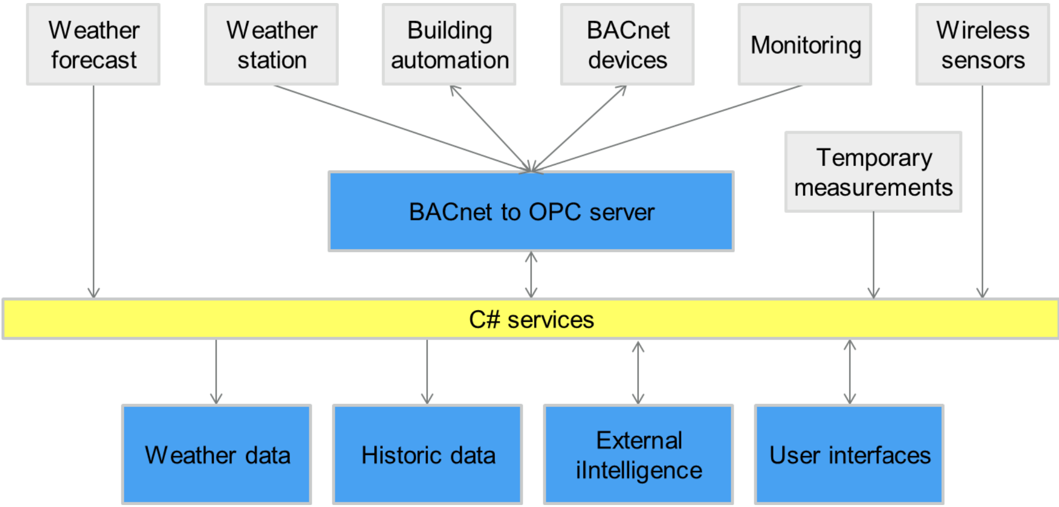

Figure 4.1: Schematic of functional principle

4.1 Monitoring principle

In order to gather detailed energy data, additional sensors are installed. These sensors are placed to extend available data from the building automation system to provide complete energetic monitoring data within four specified layers. These layers are developed in order to fulfill our monitoring purposes, further, enhanced and abstracted towards the generic energy concept within the E.ON ERC main building.

Global consumption layer - consisting of all energy and mass flows that enter or leave the building. The electricity, water and gas consumption and the transfer of ambient energy are part of this layer.

Energy conversion layer - all energy conversion related energy and mass flows are part of this layer. For every energy conversion unit inlet and outlet energy flows occur. E.g. for the heat pump these flows are the electrical energy, the absorbed ambient energy and the emitted heat flow. Furthermore, sensors that map and image the conversion and generation process internally, such as temperature, pressure, control parameters, etc. within conversion units can be grouped here under.

Energy distribution layer - flows supplied by the energy conversion system are allocated and distributed within the building. Buildings can be separated in zones, following their use, their energy distribution principle and/or their geographical orientation. For each distribution system, and for each use of the building's zones, the energy consumption has to be calculated. The distribution layer's monitoring sensors are gathering the energy flows supplied to or extracted out of these different zones.

Utilization layer - Each energy or mass flow serves to satisfy a certain need, within multifunctional buildings e.g. thermal comfort in office rooms or staff facilities, heating for test benches or cooling for server rooms. The evaluation of the need-satisfaction is the last elementary monitoring layer.

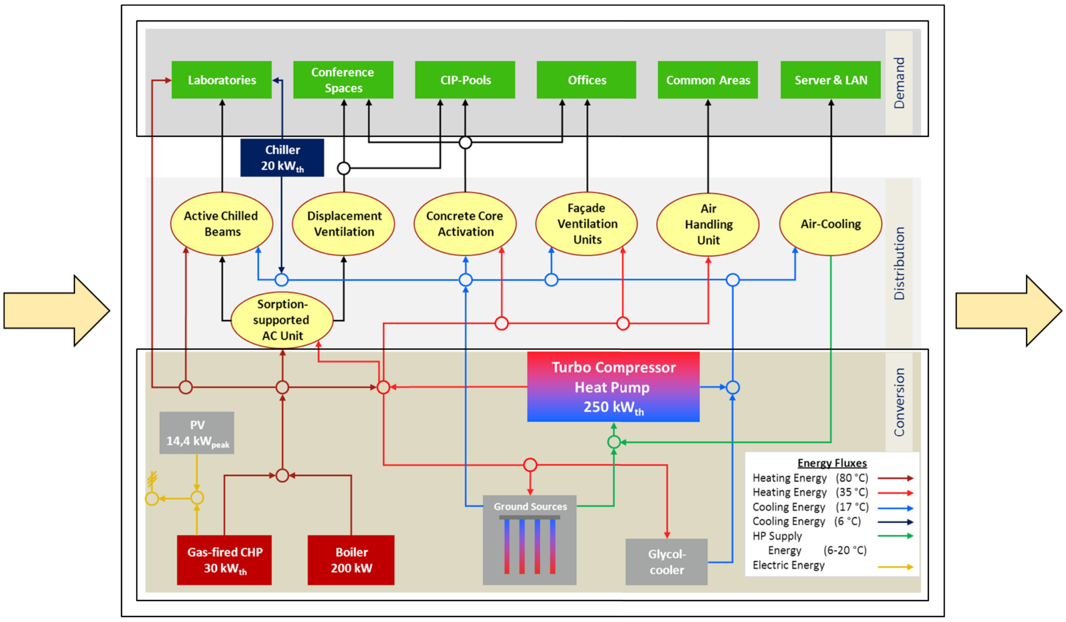

Figure 4.2: Schematic of the monitoring layers

Given physical sensor equipment at all four layers, variable and complete assessments can be conducted. These can be orientated towards different key performance indicators (KPI), distinct parts of the equipment, system interaction, user behavior and so on. At the global consumption layer, electricity flows entering the building from the grid or leaving the building due to CHP and PV production are measured. The gas consumption and the fresh water amount is observed. Furthermore, energy exchange with the environment via the geothermal field and via the glycol cooler are included. At the energy conversion layer, all energy flows entering and leaving all different conversion units are measured. KPIs of the heat pump, the boilers, the CHP unit, the chiller, and the sorption-supported air handling can be calculated. Data for other parts of the hydraulic systems, e.g. buffer storages and distribution systems is available. Concerning the energy distribution layer, each energy distribution principle, such as concrete core activation, façade ventilation displacement ventilation, active chilled beams, air handling units and circulation air coolers, is separately monitored. Distinctions between different zones, like east and west energy supply hydraulic network for façade ventilation units and the four different zones of the concrete core activation are made. The monitoring system gathers data of the ventilation mass flows for each room. All operation data of façade ventilation units, altogether 40 data points, is logged. At the utilization layer, due to the immense sensor amount that would have been necessary, ten reference rooms have been chosen to gather a representative picture. These reference rooms are equipped with sensors measuring all supplied and extracted energy flows. In every room of the building, the room temperature, humidity, CO_2 and volatile organic compounds (VOC) are monitored. Installed sensors measure the energy transfer for all special demands, such as server cooling or heat and cold supply for laboratory use.

4.2 User-added monitoring equipment

To fulfill the developed layer structure in high detail, data of the building automation system is not sufficient. Almost 300 additional sensors has to be integrated in the building. High precision magnetic-inductive volume flow meters (MID) and high precision temperature sensors are installed to calculate heat flows (refer to figure 4.3). Deeper insights into the sorption processes are provided by 14 added humidity and temperature sensors. Illuminance and presence data is gathered by wireless sensors.

(a) Magnetic-inductive volume flow sensors, different concrete core activation zones

(b) Temperature sensors, cooling supply for façade ventilation unit

Figure 4.3: User-added sensors within the E.ON ERC main building

The sensor installation is extensively validated. Each MID is put to simulation mode in order to verify right data logging. Temperature sensors are measuring heat flows as a couple. The temperature offset of each couple is measured and if larger than the sensor accuracy it is offset on the software side. An impression of this calibration provides figure 4.4.

4.3 Network topology

The new E.ON ERC main building is part of the RWTH Aachen University. The network infrastructure needed for the MCIS is integrated into the RWTH Aachen University's network topology which is expanded by two networks. The so-called monitoring network and the building management

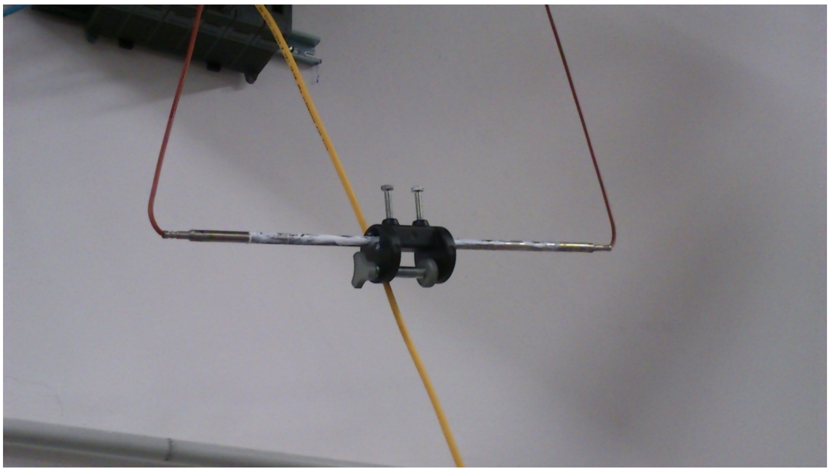

Figure 4.4: Calibration of two temperature sensors. Adjustment of sensors' temperatures towards room temperature.

network. The networks are connected to each other. Access rights can be controlled via firewalls. To administrate different users with different access permissions, a flexible virtual private network (VPN) gateway is implemented.

Figure 4.5 visualizes the network topology in high level. The office network of the E.ON Energy Reseach Center consists of all computers of the center's scientific and administrative stuff. Computers for test benches and students as well as automation infrastructure for test benches are placed within the laboratory network. The user-added monitoring hardware, the weather station, the promotional display, the wireless sensor network sink and user-added automation components are attached to the monitoring network. The building automation network is operating the management layer of the building automation system. It connects all programmable logic controllers with BACnet-components of the technical building equipment, such as the heat pump, the air handling units, and facade ventilation units. Touchscreens for direct user control and supervisory are also part of the building management network.

A cloud-based server infrastructure is installed between the building management network and the monitoring network in order to enable domain free connection to building automation components and connections to office network participants while not connecting to the building management network. For security reasons only some workstations are permitted to access the building management network directly.

MCIS databases are placed in the RWTH ICT department's intranet and redundantly in the cloud server infrastructure, which is part of the monitoring network and as well of the building automation network as mentioned above.

All components have connection to the world wide web via the intranet of RWTH Aachen University's ICT department and can also be accessed from the internet, administrated via firewall

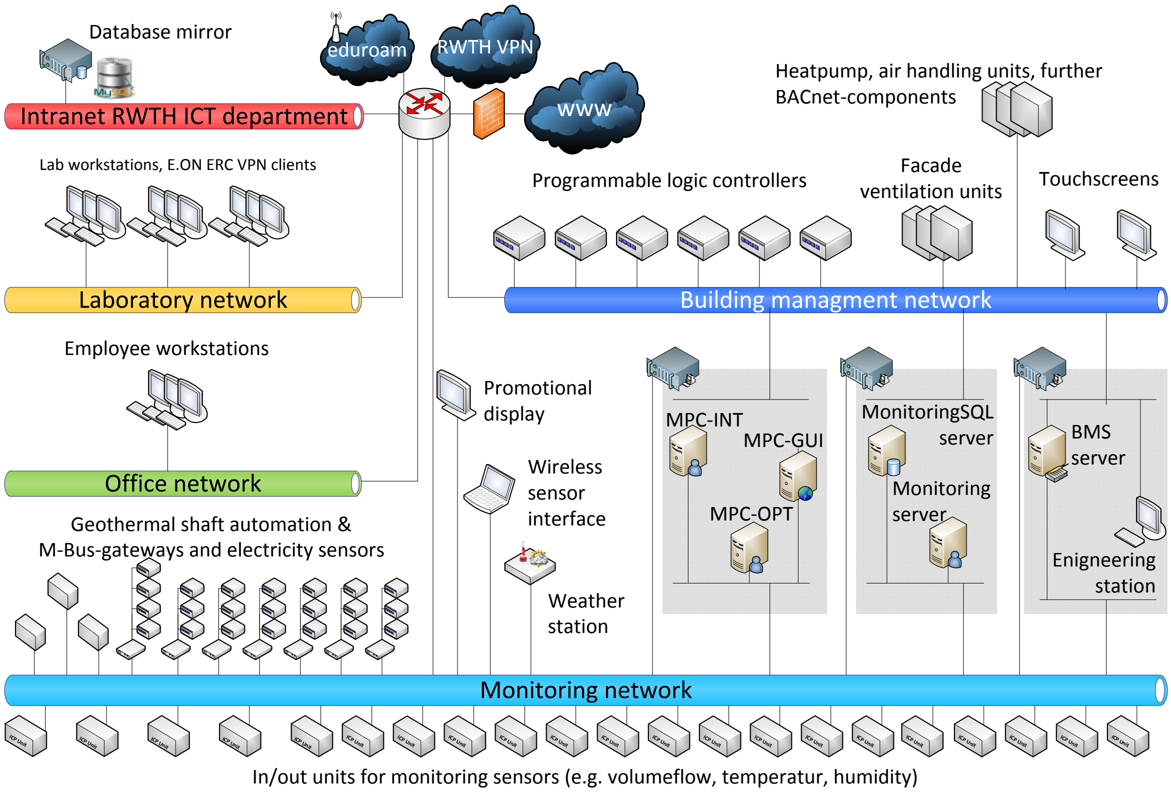

Figure 4.5: Network topology

rules. The whole building and the whole RWTH Aachen University campus offer a wireless network called eduroam and a VPN. Connecting to eduroam or to the RWTH VPN provides access to all MCIS databases hosted at the central RWTH Aachen University's ICT department.

4.4 Server infrastructure

The cloud server infrastructure between the building management network and the monitoring network consists of four VMware EXSi physical servers hosting eight plus two planned virtual machines with different operating systems.

The building management server virtual machine (BMSVM) server hosts the building management system (BMS) server. Its main purposes are operating the supervisory control and data acquisition (SCADA) system and the OPC server which serves as the main interface between external appliances and the building management system. Further, the BMS server hosts the OPC data logging service, which logs all OPC data points. Coming back to higher level, the BMSVM hosts an engineering station. All programmable logic controllers of the building automation system can be freely programmed via this engineering station. It is possible to expand the whole data network of the building automation system for any thinkable use.

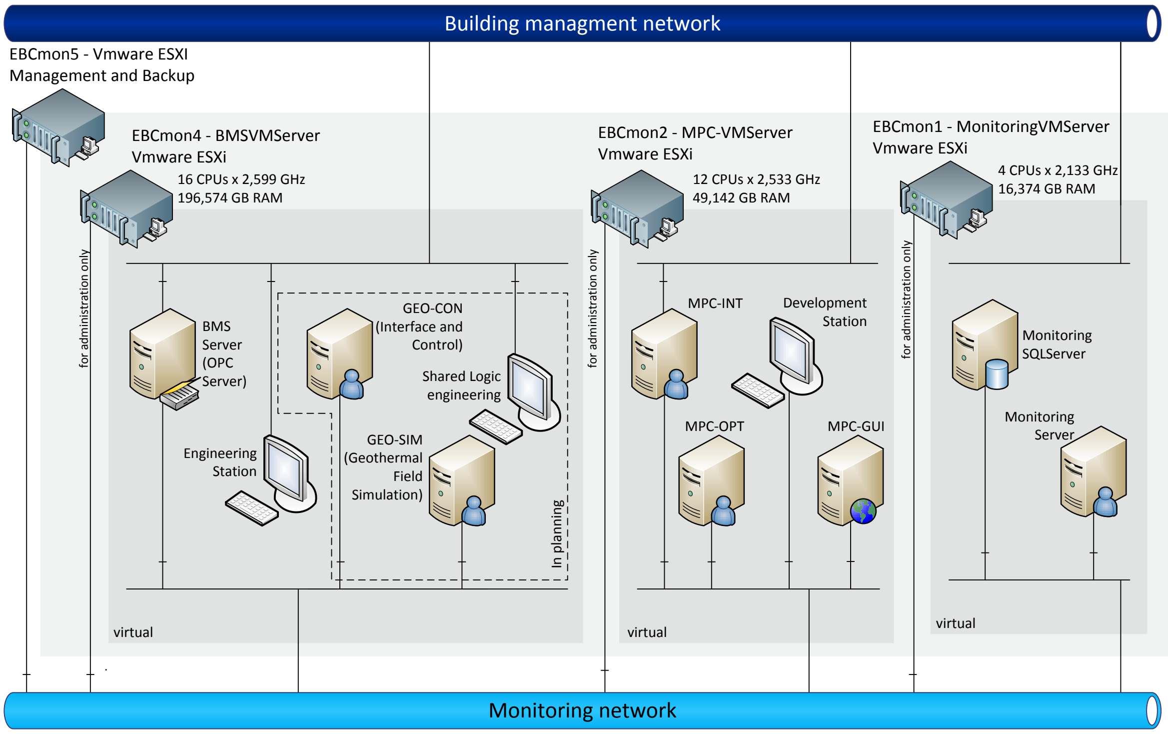

Figure 4.6: Server infrastructure

The monitoring virtual machine (MonitoringVM) server hosts two virtual machines. It hosts the monitoring server which collects data from user-added monitoring equipment and other data sources, such as weather station, weather forecast and TCP/IP sensors. It further hosts the monitoring SQL server which serves as the local database for gathered data as well as for configuration data.

The model-predictive control virtual machine (MPC-VM) server hosts three virtual machines, an interface machine (MPC-INT), providing an interface between the OPC server and the the optimization server (MPC-OPT). A further virtual machine (MPC-GUI) hosts an apache web server offering a graphical user interface for configuration of data points and system elements for model-predictive control.

The forth physical server is the geothermal virtual machine (GeothermalVM) server which hosts two virtual machines, the geothermal control and interface server (GEO-CON) and the geothermal simulation server (GEO-SIM) conducting control experiments and building coupled simulations concerning the geothermal field.

4.5 Data acquisition

Central OPC logging

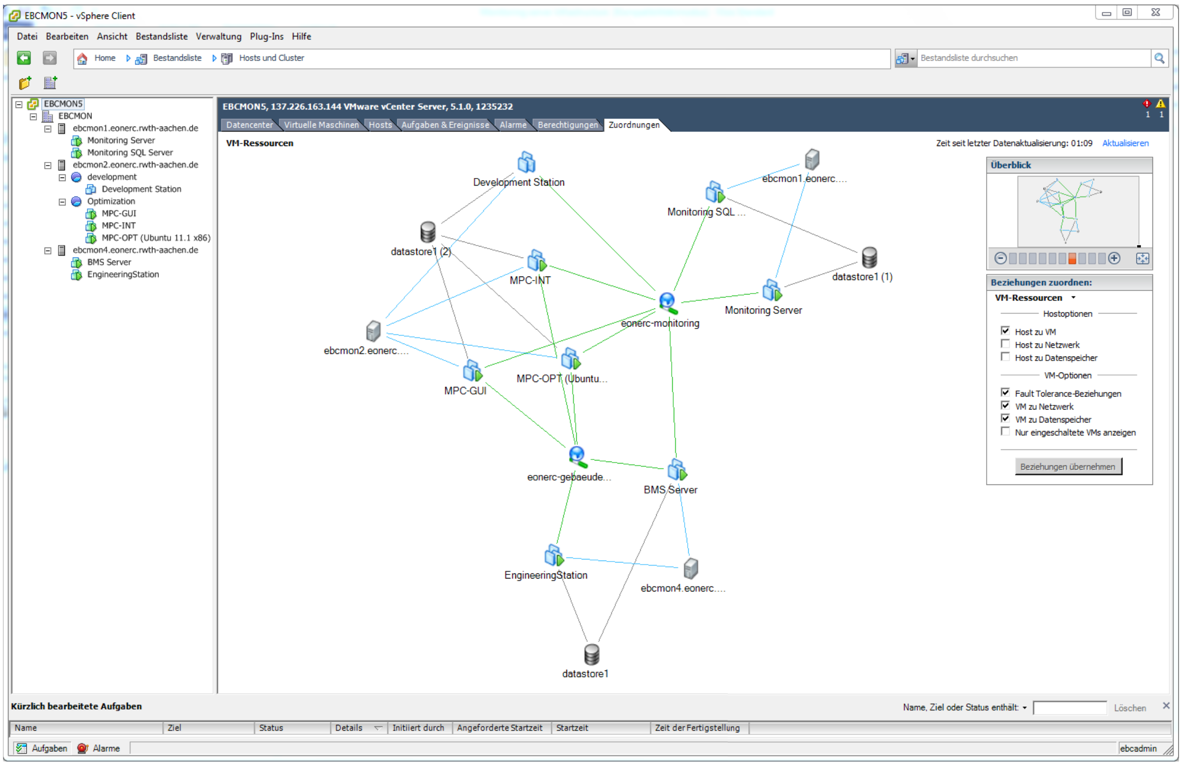

Figure 4.7: Screenshot of the virtual server infrastructure management tool

A central data logging service gathers all data points from a central OPC server. The OPC server unions data from a BACnet parser within the building management network. The BACnet parser gathers all BACnet data points from all programmable logic controllers (PLCs) and all further BACnet devices, such as façade ventilation units, heat pump, and sorption-supported air handling units. The PLCs have virtual data points for all user-added sensors. Further, they have data points for weather forecasts and for weather station sensors. A Labview-program, a weather station service and a weather-forecast service provide actual data for virtual data points to the OPC-server. The OPC-server then forwards the data to the virtual data point on the PLC level. Since the central data logging service gathers all data points within the OPC-server, the data points from the Labview-program as well as from the other services are logged this way. Concerning the PLCs, sensors and actors are connected with analog communication and in building automation commonly used bus systems as BACnet MS/TP, KNX, LON and M-bus.

User-added monitoring sensors

The above mentioned Labview program gathers data from user-added sensors via distributed in/out-units. These in/out-units use TCP/IP to communicate to Labview and analog communication to communicate to the user-added sensors. As analog sensor communication current, 4...20 mA, voltage, 0...10 V, and resistance measurement for temperature measurement are used. Once gathered, the Labview-program communicates the actual data points to the OPC server.

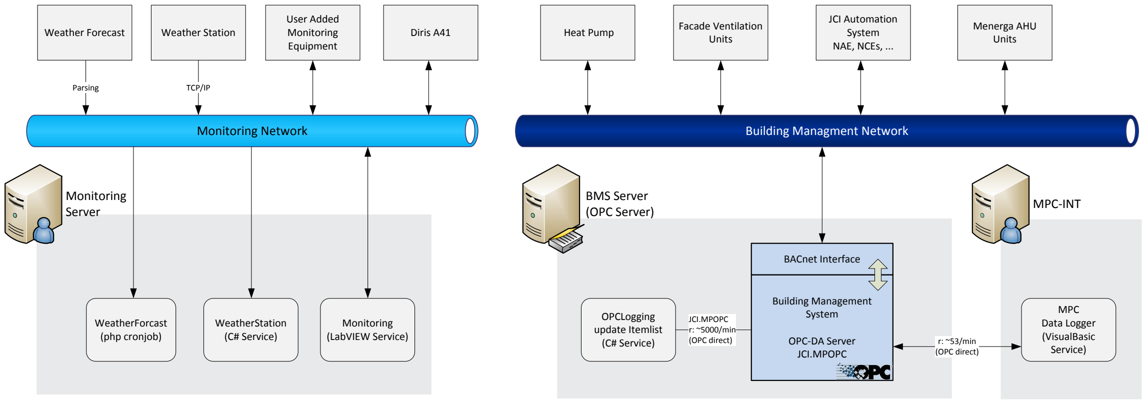

Figure 4.8: Data acquisition

Weather station

The weather station service receives real time data from the weather station via TCP/IP communication. It prepares the received string of data and publish it on three TCP ports in three different ways, first, as the data has been received, second, as prepared string with data point indication on actual data basis, and third, as prepared string with data point indication on an one-minute-average basis. It further sends the data as received and to the OPC server. Further, the service uses a SQL data base to store the weather data on an one-minute-average basis. A central document informs about the addresses of all available TCP ports.

Weather forecast

The weather forecast service gathers weather forecast data three times a day. At the moment, it gathers data from four different locations around Aachen. The service forwards the data to the OPC server and to a weather forecast data base.

Wireless Sensor Equipment

The Centre Suisse d'Electronique et Microtechnique SA (CSEM) installed, for research purposes, a wireless sensor network. This network uses an auto-routing wireless communication developed by CSEM. Hereby, each sensor communicates to its nearby sensor, which finally communicates measured data to a data sink. The sink stores the data within a pgSQL data base. The sensor network is flexible expandable.

Temporary Measurement

Within the building, researchers conduct different experiments. In order to store produced data sets in a way that they can be reused, the MCIS offers the possibility to easily import them to the central databases. The data then has a clear structure and can be found at any time. Due to different data formats, different import possibilities are offered.

4.6 Databases

The MICS has six databases, under which two databases are redundant. Two different servers host the seven databases. Figure 4.9 shows all databases available databases. The monitoring SQL

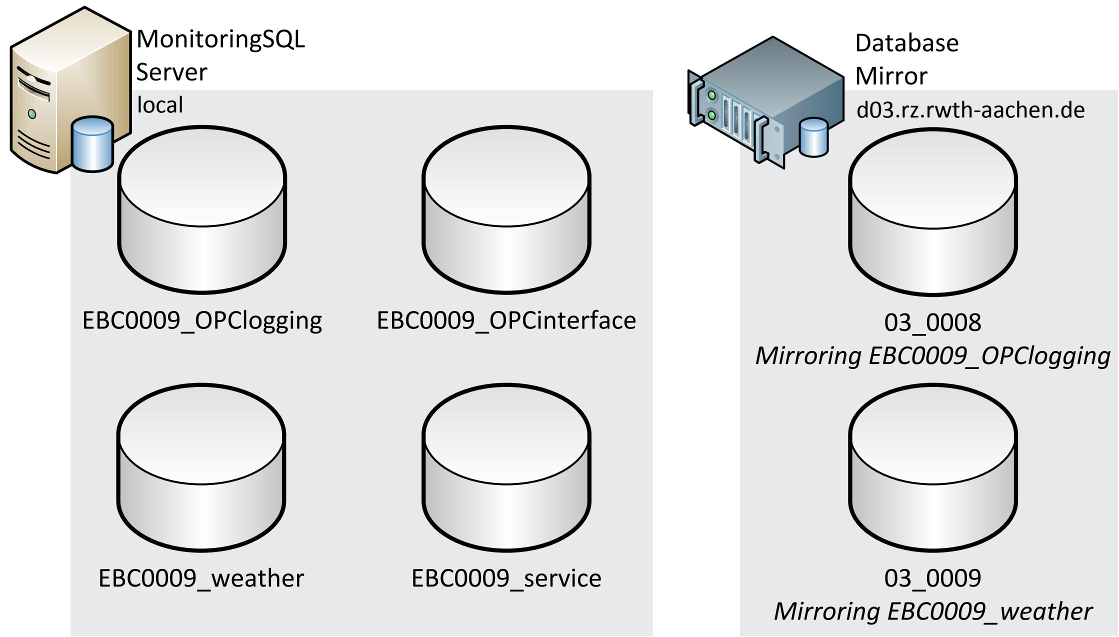

Figure 4.9: Databases

server locally hosts four databases. The data logging database, "EBC0009 OPClogging", the configuration database for an OPC-TCP-interface, "EBC0009 OPCinterface", the weather data database, "EBC0009 weather", and a configuration database for further services, e.g. a building journal, "EBC0009 service". These databases are SQL-dumped one time per day. A further backup of the SQL-server as well of the SQL-dumps is conducted once a day. For the two mirroring databases hosted at the RWTH computing center a backup is automatically conducted once a day. Data, that is often queried and that has to be accessible to different groups of users, not only for users within the RWTH IP range, is mirrored at the RWTH computing cluster. Here, access rights can be easier and more flexible arranged than within the monitoring network. IP firewall rules manage the IP access rights.

Especially, the data bases model of the data logging database is not finally sufficient. in April 2014, all data is event-based stored in a single data container. With increasing data amount the query time rises. A solution would be to have monthly separated data containers. This has to be implemented within a future task.

For long term data storage a suitable solution could be HDF5. On a monthly basis, data could be automatically exported into HDF5 data containers. This is also considered a future task.

4.7 Data analysis and visualization

Data from SQL databases can be queried from almost every software that can be used for data analysis. Tutorials and predefined functions for individual data analysis are available for Python, MATLAB and Excel. They can be found within the EBC wiki, which is a wiki-based knowledge management tool used at the Institute for Energy Efficient Buildings and Indoor Climate. Automated data analysis and visualization is done by MATLAB functions.

Basically, different software tools and programming languages are able to access SQL data bases and process data. We implemented routines for data processing in Python, Excel, MATLAB and Java in order to be as inter-operable as possible and in order to provide flexible data access for data user's preferences. The data bases are accessible via VPN through the internet. An extensive building data catalog is available for data users. This data catalog can be found inside the EBC0009-SVN repository. SVN is a subversion server system, where important documents, related to the project, are stored. The data catalog consist of a description of every data point that is available throughout the whole system. Every data point is included in a schematic which is linked from the building catalog.

Figure 4.10: Schematic of the data access and processing system with online publication

A data analysis and report generation system operates on a virtual machine in our cloud infrastructure. It generates detailed daily, weekly and monthly reports on energy consumption and key performance indicators (KPIs); from whole building scale down to every single energy conversion unit and distribution system. Reports are generated in HTML format. A cloud-based web server hosts generated reports to the internet.

Daily energy report for the building

The daily energy report for the entire building consists of an energy flow diagram, a table with additional information about the system performance and a plot with weather data.

The energy flow diagram as shown in Figure 4.11 gives an overview of the total amounts of heating and cooling energy produced and distributed in the building. Different grey types indicate the temperature levels of the energy flows, starting from cooling energy at 6°C and 17°C on to heating energy at 35°C and 80°C. The systems of energy conversion and distribution are shown together with the related amounts of energy for the day. More information about the systems can be found in a table, equally to the table shown in figure4.12, which additionally contains information about maximum heat flow, as well as maximum and minimum temperatures of the day. Another diagram,equally to the diagrams shown in figure4.12, shows the outside air temperature and global radiation that we obtain from our own weather data monitoring system.

Daily energy report for the systems of energy conversion

In order to get a deeper insight in the performance of the most important systems of energy conversion, detailed reports are created daily for the heat pump, the condensing boiler, the central heat and power unit as well as for the geothermal field.

A table gives information about total amounts of energy, maximum and minimum values of heat flows and temperatures, the operating mode and operating coefficients. Two plots show the temperatures and heat flows during the day. The report is completed by information about outside air temperature and global solar radiation.

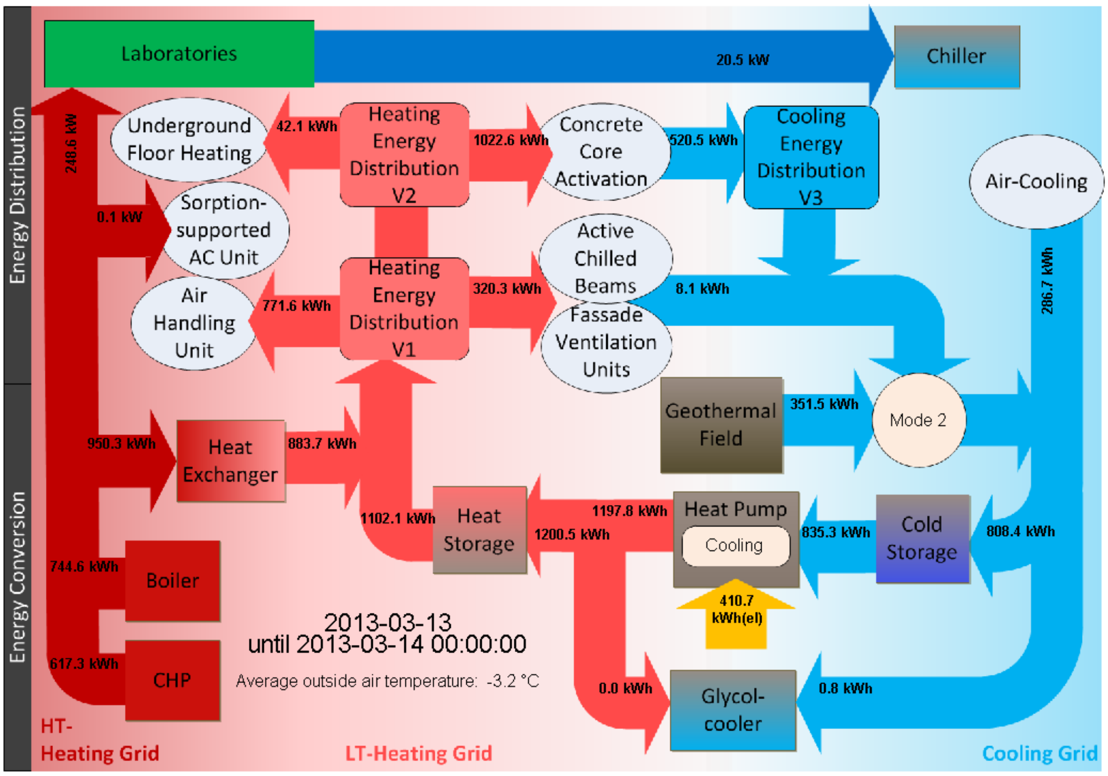

Figure 4.11: Daily building report's energy flow diagram

Daily energy report for the systems of distribution and demand

Reports about the high temperature heating, low temperature heating, and cooling energy distribution show the daily characteristics of how the energy is used in the building.

Again a table summarizes information about amounts of energy, maximum and minimum heat flows and temperatures for the day. A plot shows the heat flows going to or coming from the different systems, e.g. for the systems of low temperature heating. Additional plots display the temperatures of the flows over time and the weather conditions at the building for the day.

Monthly energy report

Once in a month a report is created that summarizes the total energy production and consumption of the building's systems. Furthermore it shows how these amounts of energy are allocated to the different days of the month. Information about the outside air temperature and the total amount of global radiation in the month completes the report.

The monthly energy reports are a basis for long time observation of the overall building performance.

Online data visualization

Online data visualization is possible via two different tools. For all OPC data points a commercial supervisory control and data acquisition (SCADA) system is used. For the user-added monitoring equipment an Labview-based user interface has been implemented.

The commercial SCADA system visualized almost real time data. Each data point can be flexible placed within schematics or component pictures. It is possible to get a quick and fast impression of the actual operation status. As user-added monitoring equipment, wireless sensors, weather forecast and weather station are forwarded to the OPC-server (please refer to section 9.6) they become available to the SCADA tool.

Especially for maintenance purposes for the user-added monitoring system, the so-called "remote control" tool offers great functionality. Actual data point values can be observed directly from the Labview data gathering service–before they are forwarded to the OPC server. The data points can be sorted by in-out-expansion unit and via in-out-modules of the ICP DAS automation system, which is used for the user-added monitoring sensors. Failures of modules and expansion units can thus be quickly identified. Further, the OPC data values of the user-added monitoring equipment can be verified and failures, during renaming or data point pinning, can be identified. Additionally, required values can be flexible chosen and are then comfortably visualized which provides an easy overview.

Promotional display

While entering the E.ON ERC main building a promotional display has been placed. It has an eye-catching design and offers flexible visualization possibilities via its 42" screen. On its backside the main components of the E.ON ERC main building's technical building equipment are graved-in.

In April 2014, a java program visualizes four data points on the promotional display: Ambient temperature, solar radiation, supply temperature of the high temperature heating grid and the indoor air temperature of the largest conference rooms.

4.8 Interfaces

Within this section, we present and sum up all interfaces of the MCIS.

FVU-Control

A web server offers control possibilities for users of each facade ventilation unit (FVU). As shown in Figure, the web server shows real time data. It is possible to choose operation modes and adjust the set point of indoor air temperature or to operate the FVU in a manual mode via setting ventilation power, heating and cooling valves, and primary and heat recuperation damp.

SCADA system

The SCADA system offers the possibility to control each implemented and writable data point manually. This tool makes it possible to operate the whole building energy system manually.

OPC-DA-Server

The OPC server is the common interface for all data access and acquisition tools. It can be used to remote control the system. It offers the possibility to design applications that are able to communicate with the building.

Read-on-demand-and-write interface, "TCP-OPC-interface"

We want to communicate in two directions with the building automation system. We want to read and write values in real time. Since our OPC server is not able to establish mass-multiple connections in parallel, we built an “OPC2TCP-interface”. Web applications, smartphone applications and many software tools can communicate via this interface. The interface is hosted in the installed cloud infrastructure.

Weather station service

The weather station service offers three TCP ports. It provides the weather station’s original TCP string, a processed and formatted string with a two second sampling rate, and a processed and formatted string with one minute averaged values.

4.9 Advanced control strategy demonstration bench

The MCIS provides the opportunity to easily set up specific environments for different experiments. In the following, we present the usage of the MCIS towards different applications. First, model-assisted control parameter fine tuning; second, model-predictive control, third, adaptive control parameter fine tuning; fourth, a thermal storage experiment.

4.9.1 Model-assisted control parameter fine tuning

Within the Positive Energy Buildings thru Better control dEcissions, PEBBLE (see section 6.2.3), project we use the MCIS to demonstrate a model-assisted control parameter fine tuning algorithm. We set up the experiment environment for the PEBBLE system, which consists of an interface server and an optimization server within our cloud environment. Special PEBBLE services have been developed within the project together with different partners. A weather forecast service gathers the weather forecast, a data logger logs only experiment design relevant data points into the experiment data base and an interface service allows for communication between the algorithm itself and the building. The interface service uses direct OPC connection to communicate with the building. Fig. 6 shows a schematic of the experiment set up Constantin et al. [2013].

The system reliably operates using the following software versions: ubuntu 11.10 as an operating system; Dymola 7.4 as simulation environment; MATLAB 2011b as optimization environment; BCVTB 1.1.0 as coupling between MATLAB and Dymola. Please refer to section 5 for more details regarding the used software.

We use the PEBBLE system to fine-tune set points of two energy distribution systems for office rooms. The algorithm fine-tunes for each office individually the room temperature set point for façade ventilation units and it fine-tunes globally the set points of a four point heating curve within a concrete core activation zone. The experiment's scope is 39 office rooms, orientated north-east and north-west and the building's concrete core activation zone north Constantin et al. [2013].

The addressed control problem is the minimization of the cost function for the energy demand. Façade ventilation units and concrete core activation deliver thermal energy. The main constraint is thermal comfort. For the quantification of thermal comfort we use the Fanger's Predicted Percentage Dissatisfied index [Fanger, 1970].

Figure 4.14 and Fig. 4.15 illustrate exemplary experiments results for the PEBBLE-controlled room. The system dynamically adjusts the set point for the façade ventilation unit within a bandwidth of 22° C to 25° C. It reacts to changing user occupancy, varying ambient temperature condition and varying global radiation. Further calculations show that it successfully maintains the thermal comfort within its constraints.
Fig. 8 presents the energy consumption of the PEBBLE-controlled room in comparison to room on the same floor where the default control strategy was used. The demonstrated algorithm leads to a lower total energy consumption, mainly due to the reduction of heating and cooling energy distributed via the façade ventilation unit. Further results and a detailed discussion can be found in Constantin et al. [2013].

The PEBBLE server infrastructure has been set up in the MCIS' flexible server environment. The MCIS' data logging enabled the evaluation of the PEBBLE experiment. PEBBLE's performance was assessed by the MCIS' automated data processing and report system.

4.9.2 Model-predictive control

We will demonstrate model-based predictive control for the geothermal field as part of a project financed by the German Federal Ministry of Education and Research (funding code 03ET1022A). This experiment is shown in figure 4.16. MATLAB runs a control algorithm which takes historical, actual, and future data out of the MCIS' data storage using SQL queries. The algorithm provides historical, actual and future data as input for a simulation. Having found a good-enough solution related to a cost function, the algorithm communicates the set of control parameters to the building via the MICS' read-on-demand-and-write interface. This time discrete process is continuously operated.

The geothermal field has 40 borehole heat exchangers. Depending on how we combine the heat exchangers they exchange more or less thermal energy. First, we analyze operation of the heat pump and decide whether more or less heat is needed. As outcome a certain combination of borehole heat exchangers is preferable. With the help of a Dymola/Modelica model we calculate the pressure drop optimal control valve angle for each heat exchanger. The results are then communicated to the BAS. The MCIS enables this experiment with its flexible server infrastructure, its data logging and report system, its read-on-demand-and-write interface, and, finally, MCIS is used for PLC reprogramming.

4.9.3 Adaptive control parameter fine tuning

Within the project Local4Global we develop, implement, demonstrate and evaluate advanced adaptive control parameter tuning algorithms with special emphasis on the development of a control system that require the minimum possible infrastructure. More precisely, we consider the adaptive control design of buildings or systems of buildings, where there is no or little communication between the sensors of neighboring offices/rooms or buildings. The main advantage of such control designs is that there is no need for the deployment of an expensive sensor network infrastructure that will "connect" all system sensors. The local sensors, instead, are used in order to "extract" information not only from the offices/rooms/buildings they reside but also from the neighboring ones. Moreover, an "expensive to develop and maintain" model of the building dynamics will not be needed, a prerequisite in the majority of existing building climate control systems et al [Italy, 2013.]. The MCIS provides the optimal demonstration bed.

Figure 4.17 shows the experiment set up. First, we choose a specific control system with, e.g. a proportional-integrative-derivative (PID) controller. Via the PCL programming server we promote all control parameters, such as time, proportional, integrative and derivative constant, to the management layer. The MCIS logs the all promoted values and makes them writable. A MATLAB instance runs on the experiments server. It accesses the MCIS' data base and tries to find advantageous control parameters. The result, a set of control parameters for a certain controller is finally communicated to the building using the MCIS' interface. The adaptive tuning algorithm is operated within a development environment and can be flexible changed and continuously improved. The algorithm optimizes controller without using simulations. Experiments observation and evaluation is conducted by MCIS' data processing and automated reports.2

4.9.4 Thermal storage experiment

The focus of this analysis is the evaluation of energy storage in building's thermal mass, comparing a conventional radiator heating with concrete core activation (CCA) as heat distribution system. Therefore, within an accurately monitored room at our research center a field study was performed and the results were compared to simulation outcomes of a thermal model for the same room. Since the behavior of the simulation model proves to be close to the thermal behavior of the real room, the model is then used to simulate a scenario for activation of the building's thermal mass according to a signal describing the availability of renewables.

For both systems a three hour overheating phase allowed to postpone further heating demand in winter by more than eight hours. The radiator based system lead to a room temperature increase of 3.1 K compared to only 0.2 K for the CCA. Thus, due to potential thermal discomfort the radiator based system would require either the limitation of permitted indoor temperature or a more complex control with occupancy monitoring / prediction. Furthermore, it is shown for the CCA system, that integration of an exemplary signal indicating high availability of renewable energies (RE) would have doubled the consumption of RE during our field test time, without compromising thermal comfort [Wolisz et al., 2013].

To conclude this chapter, we state that, the potential of the demonstration bench is extraordinary. An automated data analysis provides direct information about what is currently happening in the system and what are the consequences. We can flexibly set up experiment infrastructures for different types of control approaches. The design of each experiment is free in terms of detail and scale. The MCIS enables flexible demonstrations and flexible field experiments for research towards advanced rule-based control, agent-based control, model-based predictive control and adaptive control in building energy or heating, ventilation and air-conditioning (HVAC) systems.

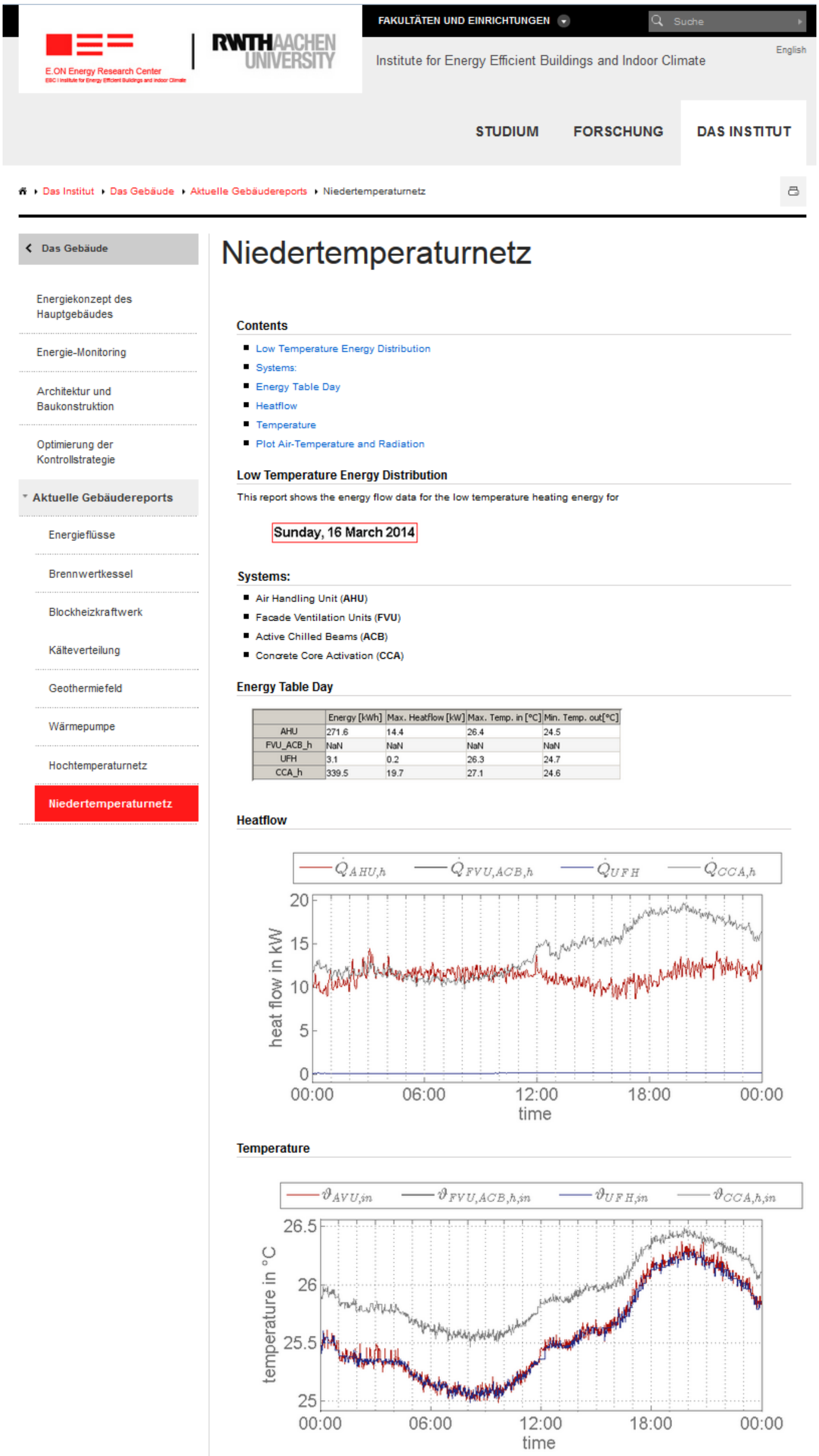

Figure 4.12: Exemplary monitoring report; screenshot from E.ON ERC's homepage

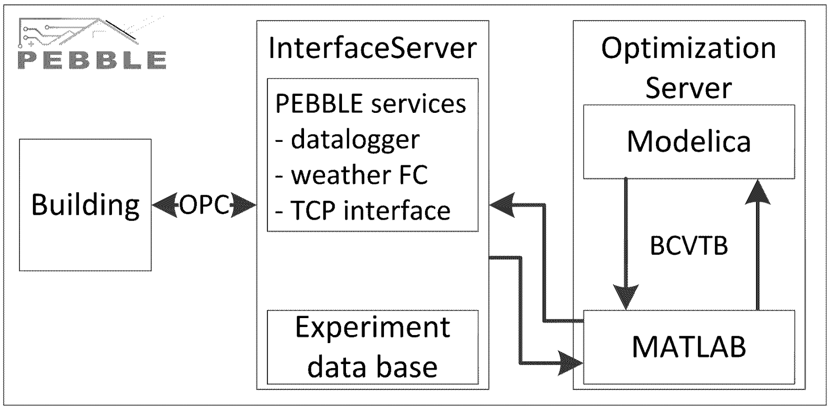

Figure 4.13: Configuration for PEBBLE experiments

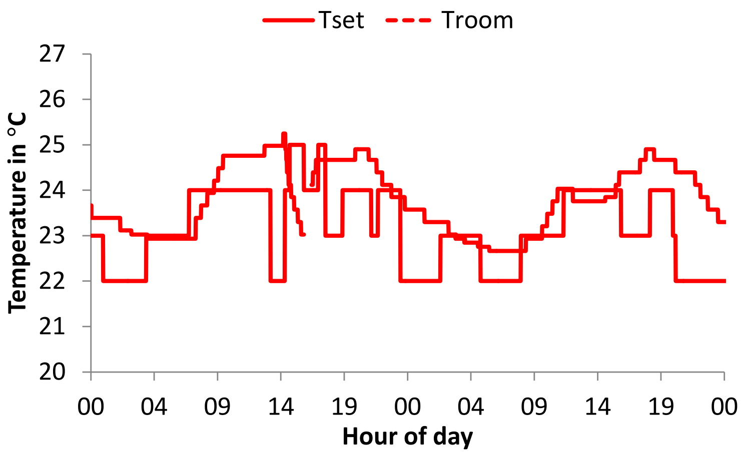

Figure 4.14: PEBBLE set temperature and actual room temperature

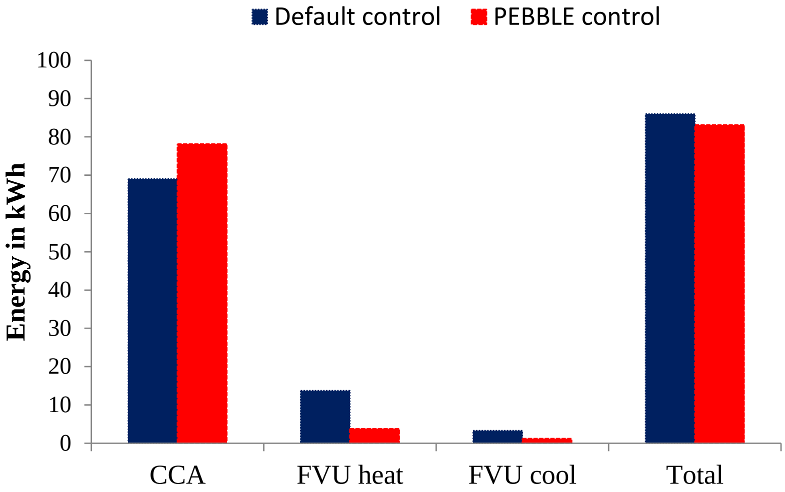

Figure 4.15: Energy consumption in a PEBBLE controlled room versus energy consumption in a conventional controlled room

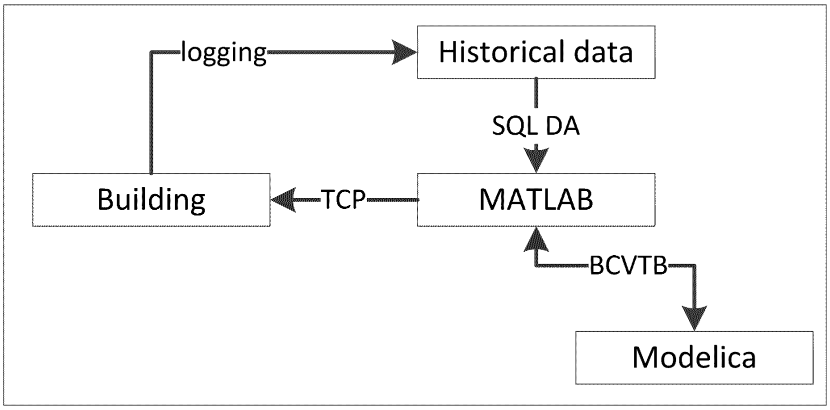

Figure 4.16: Experiment setup for model-based predictive control within the geothermal field control project

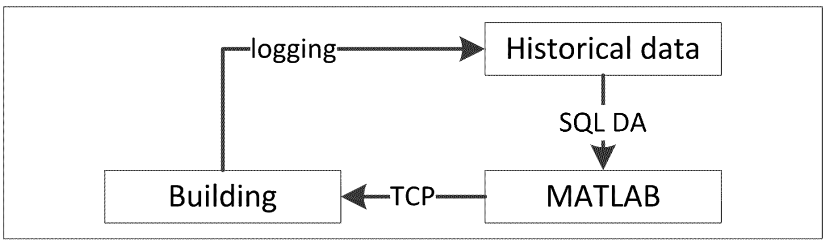

Figure 4.17: Experiment setup for external adaptive control parameter fine tuning without simulation within Local4Global project

5 Modeling and Simulation

This chapter presents the developed models for the building and the building system engineering. As the building is quite large, having both central (e.g. for common areas) and distributed (e.g. for office rooms) air conditioning systems it was necessary to develop several thermal building models with different degrees of detail to tackle each of this cases individually.

For building the models and setting up the simulation we used the modeling language Modelica [Modelica Association, 2011] and the simulation environment Dymola [Dassault Systems, 2011]. For developing and testing control strategies for the different pieces of technical equipment MATLAB and Simulink [MathWorks, 2012] were used, along with a proprietary development environment for the façade ventilation units, which lead to setting up co-simulations between these tools. For the co-simulation we used one one hand our own *C#* interface for HTTP-request and on the other hand the BCVTB (Building Controls Virtual Test Bed) software [Wetter, 2009].

For each model a short description of the modeled physical processes along with known limitations of the model are provided. Afterwards a model evaluation, either by comparison with standards or with measurements, is presented.

5.1 Thermal building models

Several models were built for the E.ON ERC main building, using the components of our own *Building* - Library [Müller and Badakhshani, 2010]

- detailed office models for offices with one and two outer walls, with and without integrated conditioning systems
- a low order model for an office with one outer wall and an ideal heater cooler
- detailed tower models (three office rooms on top of each other) with integrated conditioning systems
- zone models, where multiple rooms with the same usage are aggregated

For the detailed as well as the zone models each relevant component (walls, windows, shading and doors) are modeled individually. With the exception of the low order model, the room models consider the following physical processes:

- transient heat conduction through walls; each wall consists of several layers with different physical properties; further discretization of each layer is possible

- steady-state heat conduction through glazing systems; transmission of short wave radiation through the window depends on a constant coefficient or depending on the solar incidence angle; transmitted radiation is considered together with the radiation from room facing elements
- radiative heat exchange to the environment
- heat convection at outside facing surfaces either with a constant coefficient, depending on wind speed, or depending on wind speed and surface abrasiveness
- heat convection at inside facing surfaces depends on the wall orientation and the temperature difference between the room air and the wall surface
- radiation exchange between room facing elements
- temperature balance equations for the room air volume; per room only one air node is considered; humidity is not considered in the air node

The incident solar radiation on tilted surfaces is calculated using a isotropic sky model [Duffie, 2006].

All outer walls are whole walls connected to the room air and the ambient, while inner walls are half walls, each half belonging to one of the rooms which share the wall. Airflow among rooms is not explicitly considered.

We decided on two ways for evaluating our models: by evaluating the components with a standard and by comparing the specific room models against measurements.

5.1.1 Evaluation of a room model with the ASHRAE 140

For the evaluation of the components against a standard we chose the widely used standard ASHARE 140: Standard Method of Test for the Evaluation of Building Energy Analysis Computer Programs [ASHRAE 140]. The standard defines a series of comparative test cases, with focus on the building thermal envelope and fabric loads. The tests are divided into two groups *basic test cases* and *in-depth test cases*. Each of the mentioned groups contains low mass and high mass cases: test cases 600 to 650 represent a building with low thermal mass, and test cases 900 to 960 represent high thermal mass. For additional information on material properties of the low and high mass building as well as the particularities of each test case refer to the standard.

The base building, as shown in figure 5.1 is a rectangular room with a 48 m^2 floor area and two windows each with an area of 6 m^2 on the wall facing south.

All test cases are simulated with one to eight established simulation programs and the relevant simulation results are given in graphical and tabular form. These results, along with the differences in results between test cases (sensitivities) are used for the evaluation of the own software kit. For each test case several outputs are evaluate, but the most widely used between the cases are:

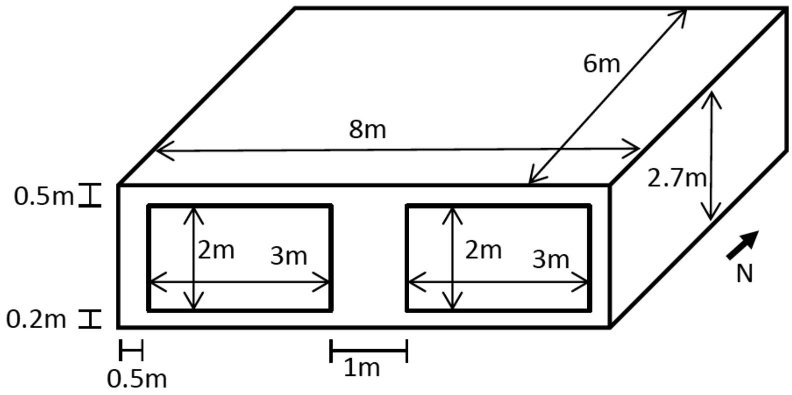

Figure 5.1: Main room model used for testing in the standard ASHRAE 140

- annual heating load in kWh
- annual cooling load in kWh
- hourly integrated peak heating load in kW
- hourly integrated peak cooling load in kW

In order to facilitate an easy evaluation of different outputs, over different test cases we introduced a benchmark diagram. For generating the benchmark diagram, the minimum and maximum values of the given simulation results in ASHRAE 140 are used. In order to illustrate all test cases of each category in one diagram, the minimum, maximum and our own results were divided by the median values of all given simulation results for each test case in the standard.

Figures 5.2 exemplary presents the benchmark diagram for the annual heating load.

The results for our model are always between the maximum and the minimum of the results obtained with the other softwares. It is important to note that the evaluation with the standard improved the models, most notably the transmission of solar radiation through windows and the radiative heat transfer towards the outside. The set of models from the *Building* library are thus considered to have been successfully evaluated with the standard ASHARE 140.

5.1.2 Evaluation of a room model by comparing with own measurements

The evaluation with the standard assures us that the components we use to build up a room accurately describe the relevant heat transfer processes. However the standard provides exact information about material data, boundary condition and function mode of the technical equipment. In a real building such data is bound to be inexact. In order to reduce these uncertainties and test the models in regard to the technical equipment installed, we built our own measurement set-up.

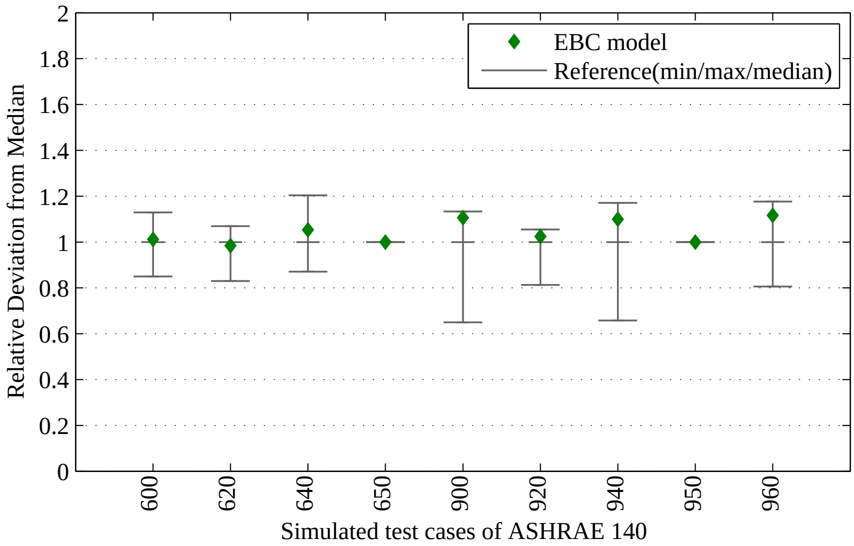

Figure 5.2: Annual heating load for basic cases

The measurements were performed in an office over one winter week in 2013. The room is a corner office with a floor area of 41 m^2, two external walls (north-east and south-west orientation) and with a total window area of 24 m^2. The room was unoccupied, the blinds were left shut for the first part of the experiments, and drawn up for the second. The office room is conditioned using concrete core activation within the ceiling, which is supplied by a heat pump. Figure 5.3 shows a picture of the room taken with a thermographical camera, which we used to compare two types of measurement for the surface temperature. The picture is relevant in that it shows the temperature difference between the ceiling and the other surfaces in the room. This aspect along with the slow dynamic introduced into the system by the concrete core activation first heating up the wall from the inside and then the room makes the experiment very relevant as such a case was not covered in the ASHRAE 140.

As the considered office is a reference room in the building, it is equipped with additional monitoring equipment, measuring the supply and return temperatures as well as the volume flow in the concrete core activation. Additionally six tripods with air temperature sensors at four different heights were set up in the room, according to the ISO 7726 standard [DIN, 2002]. The ceiling surface temperature was measured at three positions. Figure 5.4 shows the positioning of the sensors in the room.

An electrical radiator with a maximum power of 2.0 kW was used to represent a conventional radiator based heating system for comparison with the concrete core activation. The total electrical consumption of the set-up consisting of radiator and measuring equipment was constantly measured. Weather data (outdoor air temperature, wind speed, global and diffuse solar radiation) is

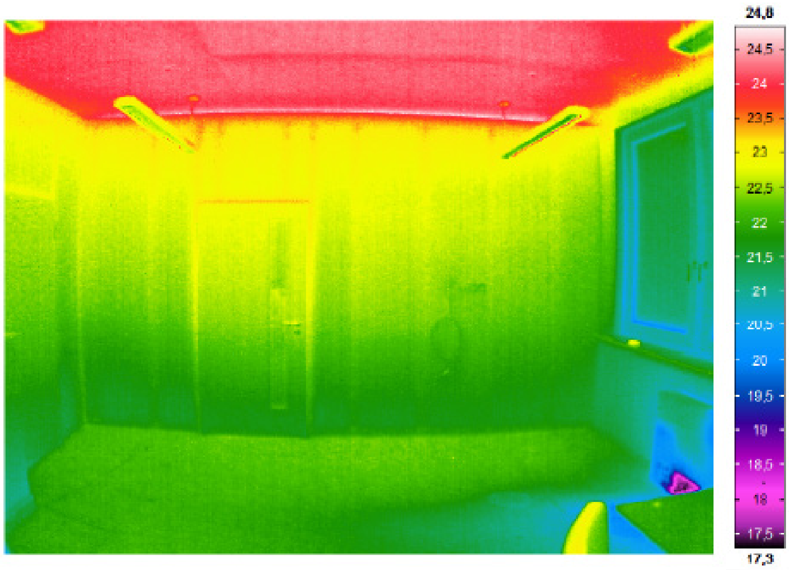

Figure 5.3: Thermography view of monitored office room

available from our own weather station, situated on the roof of the nearby experimental hall.

At winter conditions (ambient temperatures in range of 3 °C) the test room was repeatedly overheated for approx. three hours with the maximum power of either the concrete core activation or the radiator system. Afterwards the cool down period followed.

The gathered temperature values from all sensors are aggregated to an average temperature value for the room temperature. Also, based on three sensors, an average surface temperature of the ceiling is calculated to monitor the status of heat stored into the concrete.

Figure 5.5 shows the comparison between the simulation and measurement results for the room air temperature during a five day phase of the field study. The increase in the air temperature on the first day is due to overheating with concrete core activation. The following four peaks are results of overheating with the radiator. At a first glance we recognize that the simulation follows a similar trend to the measurements and an overall similar temperature level.

When doing a more detailed analysis of the results over the whole period of the experiments we obtained for the room air temperature a mean biased error (MBE) of 0.0676 and mean absolute error (MAE) of 0.4512. We consider these results satisfactory.

5.1.3 Simulation of multiple rooms

At the beginning of the project, the whole building was zoned according to usage and control strategy. Simulations were carried out for the whole building, as well as separately for each zone with

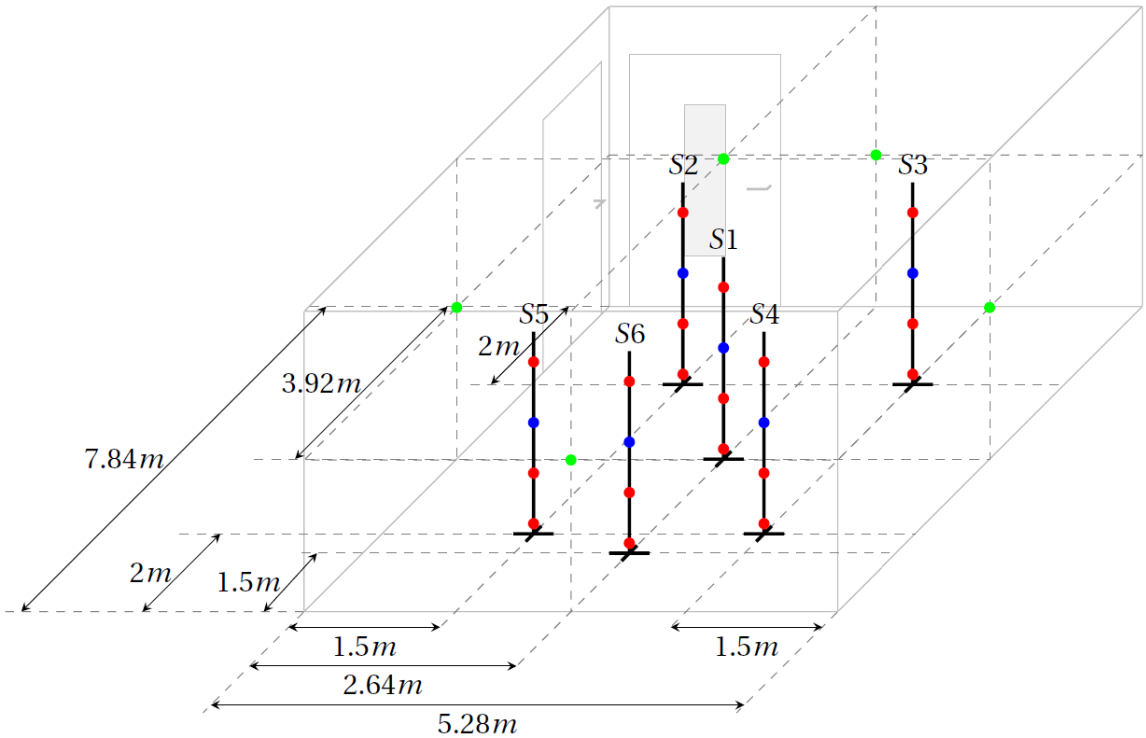

Figure 5.4: Sensor positioning in the monitored office room

adiabatic boundary conditions to the neighboring zones in order to asses the introduced differences. Zones with the same functionality, and as such the same principles of heating, cooling and ventilation, are usually grouped together on a floor, whereas the floors themselves usually have the same spatial distribution for their computer rooms, offices, and conference zones. Thus the assumption of adiabatic boundary surfaces is a realistic one, and the errors are expected to be small. Figure 5.6 shows the simulation results for one zone from the simulation of the whole building and from the simulation of only one zone. Both simulations start from a steady state and show a free floating character. The maximum difference is of about 0.5 K.

Further complications arise however, when addressing the control problem. As it happens for example in the case of office rooms, where both the concrete core activation system, stretching over a whole zone, and the façade ventilation unit as a decentralized unit are present. As we control each room temperature individually, each room has to be modeled in detail. However such a simulation model would lead to very long simulations, so simplifications need to be made.

As the building is well insulated and all the offices have a similar use, we assume the main factor that differentiates them is their orientation. So instead of simulating all rooms, only exemplary rooms with different orientations are simulated. To this purpose we build *tower* models. A tower stretches over all floors of the building and thus has three rooms, on top of each other, one on each floor. The boundary conditions toward neighboring offices are considered adiabatic. Figure 5.7

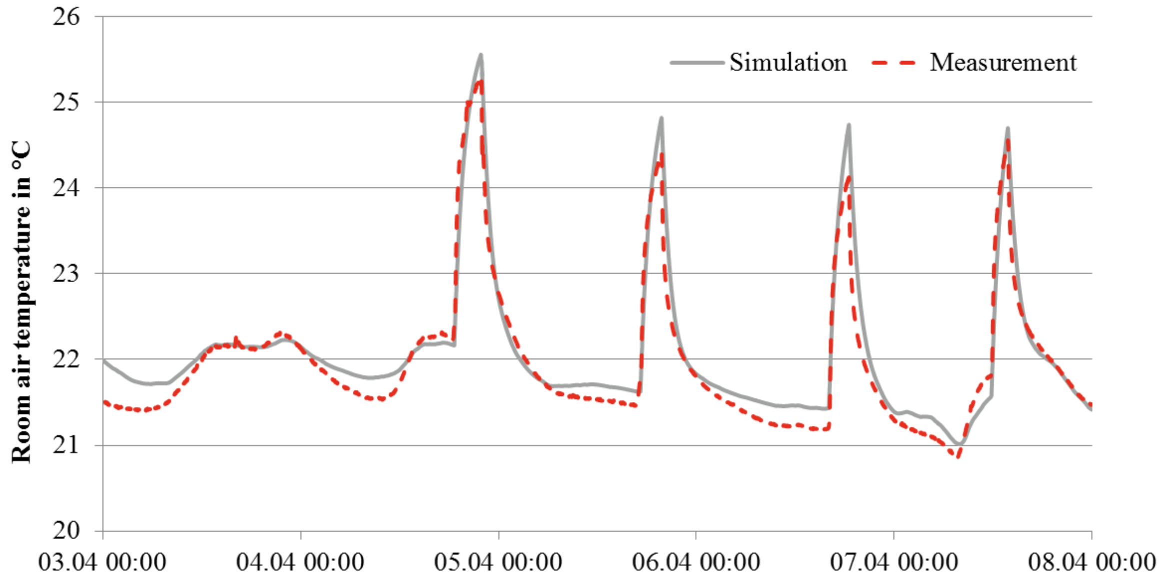

Figure 5.5: Comparison of simulation results with measurements

shows the name and the orientations of the resulting three towers when considering the concrete core activation area north of the building. While the results for Tower Corner can be used only for these rooms in the real building, the results for the other two towers can be used for all the rooms with that orientation.

5.1.4 Low order models

The last type of models built were the lower order models, which we used for obtaining a state space representation of the room model, to be used for testing algorithms of model predictive control. The low order model is actually a third order model, considering three capacities, and as such three states:

- temperature of the outside wall (all outside walls aggregated in one component)
- temperature of the inside wall (all inside walls aggregated in one component)
- temperature of the air node inside the room.

For more detail regarding the used model refer to Lauster et al. [2014].

The low order model was built for an office room. We will detail here the main parameters of the room, as well as the assumptions regarding internal gains, as these were consistent throught all the experiments. This room is situated on the first floor. The room area is 18.75 m^2 and the windows have an area of 8 m^2. The boundary conditions at the interior walls are considered as adiabatic.

The room has been designed for two persons. In order to account for interior loads, persons, machines and lightning are considered. The heat load of the persons which depends on their activity

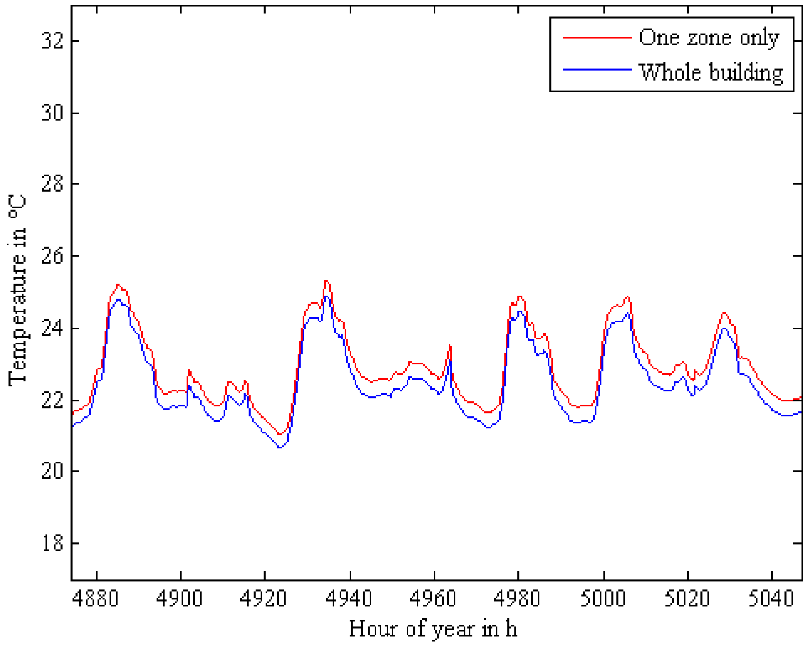

Figure 5.6: Comparison of simulation with the whole building and with only one zone

and room temperature are calculated according to VDI 2078 [VDI, 2012]. The convective share of heat emission is 0.5. The heat emission of the machines is determined according to DIN V 18599, [DIN V 18599], with a 0.6 convective heat ratio for lightning the concurrency factor is set to 0.3, the maximum value is 24 $\frac{\mathrm{W}}{\mathrm{m}^2}$ with an convective share of 0.5. Interior loads are regarded only during working hours (9:00 to 18:00, Monday to Friday). The CO_2-emissions for each person is 17 $\frac{\mathrm{l}}{\mathrm{h}}$.

5.2 Models for the technical equipment

For the technical equipment numerous models were built, some as part of this particular project, some as part of related projects. All existing relevant models will be presented here, in order to give a complete description of the available models for:

- the conditioning of an office room: concrete core activation and façade ventilation unit
- a heat pump system
- a boiler and a CHP
- a central air conditioning unit
- a geothermal field: for short and long term analysis

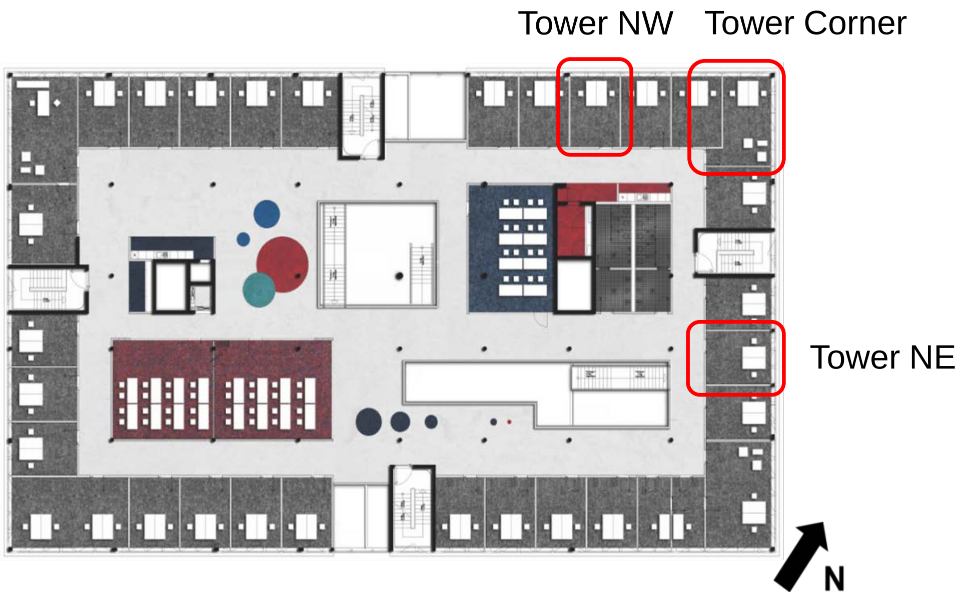

Figure 5.7: Exemplary towers for the concrete activation area north

5.2.1 Heat pump system

The heat pump system of the building consists of three main components (see figure 5.8)

- heat pump
- hot water storage
- cold water storage

For each of these components models were built in Modelica / Dymola. Additionally the control strategy of the pump was implemented separately in Simulink. The model for the heat pump is

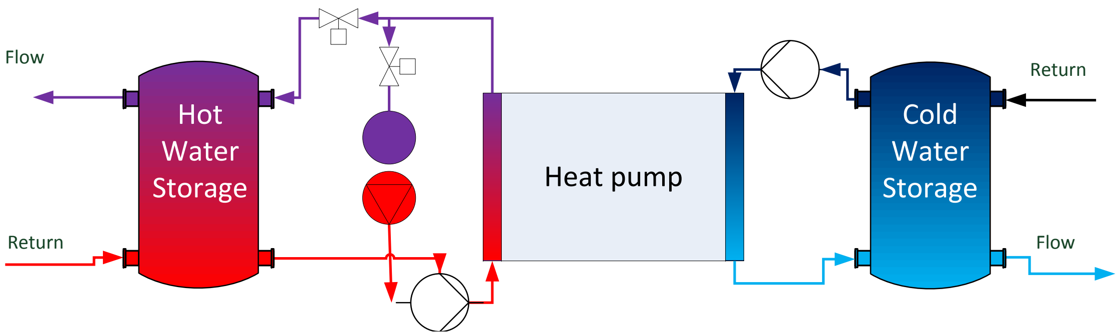

Figure 5.8: Schema of the heat pump system

a black-box model, as the refrigerant circuit is not build explicitly, but modeled using polynomial functions. Depending on the source and sink temperatures, as well as the rotational speed of the compressor, the generated thermal power is calculated. The polynomial function is generated by analyzing the characteristic diagram of the heat pump. However in our case no such diagram was available, so we made a compromise by using existing available characteristic diagrams:

- heat pump with similar maximum and minimum power (HP1). However this data was only available for maximal rotational speed.
- heat pump with a characteristic diagram depending on rotational speed (HP2).

The following equation is used to calculate the power output of the heat pump $\dot{Q}$ as a function of source temperature T_Q, sink temperature T_S and rotational speed n:

$$\dot{Q}(T_Q, T_S, n) = \underbrace{\dot{Q}_{max,HP1}(T_Q, T_S)}_{\text{maximal power}} \cdot \underbrace{\frac{\dot{Q}_{max,ownHP}}{\dot{Q}_{max,HP1}}}_{\text{scaling factor}} \cdot \underbrace{\frac{\dot{Q}_{HP2}(T_Q, T_S, n)}{\dot{Q}_{HP2}(T_Q, T_S, n_{max})}}_{\text{rotational speed factor}} \tag{5.1}$$

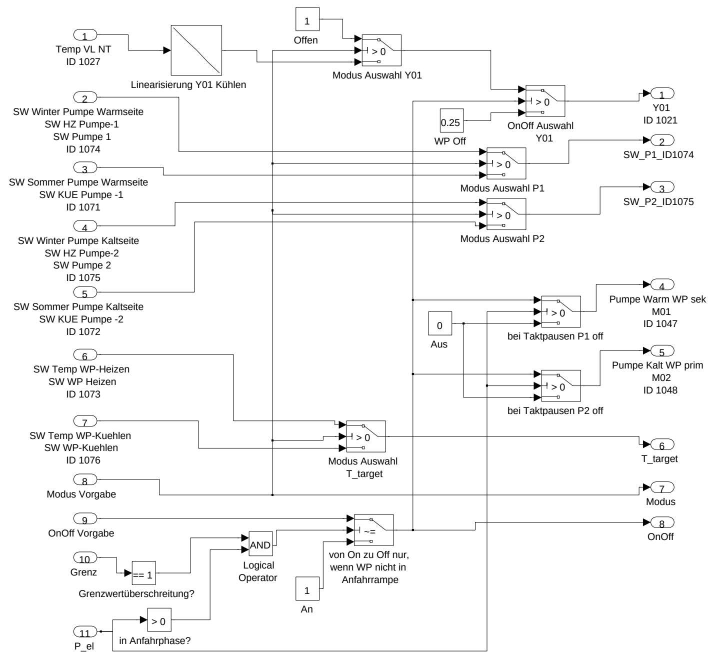

Figure 5.9: Control of the heat pump system modeled in Simulink

The control strategy for the pump was build in Simulink. It was adapted from the existing control strategy, implemented by the engineering firm, which was commissioned with the automation of the building. The control was implemented using a dedicated proprietary software and made use of the firm's own blocks, e.g. an adaptive PID controller. This implementation was first stripped of unnecessary loops that had no influence on the simulated model and then modularized in order to better distinguish the different functions, e.g. heating or cooling mode, set flow temperature control. For the blocks which had no direct correspondent in Simulink, blocks that most matched the functionality were used. Figure 5.9 shows the final Simulink model.

However the internal control strategy was not visible for us, meaning it was not clear how the rotational speed and hence the electrical power are adjusted in order to achieve a certain set flow temperature. Statistical analysis of the flow and return temperatures of the heat pump against the outdoor temperature did not reveal the existence of a heating curve, or of a on/off hysteresis for the set flow temperature. A solution was found to achieve a similar on/off behavior of the pump and the results are shown in figure 5.10. The solution is based on a linear dependence of the turn on and turn off times on the current energy demand of the system, derived from analyzing the measurement data. A quantitative analysis of the results is only marginally possible, as a dynamic

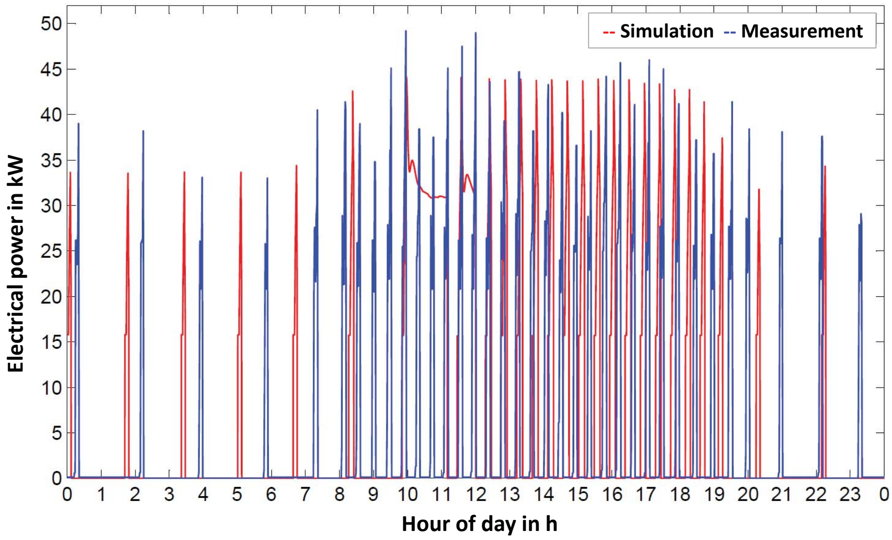

Figure 5.10: Validation of the electrical power output for the heat pump

time delay occurs between the measured data and the simulated data. However the average values for the duration of on and off modes are comparable, as is the total electrical energy consumed. We consider the model to be a satisfactory.

The model for the buffer storage is a physical model for a cylindrical component. The volume of the storage is discretized axially in layers. Each layer element has a homogeneous temperature. The heat transfer between layers takes place through heat conduction between the layers and through forced convection caused by the flow of the medium through the storage when loading and unloading the storage.

5.2.2 Boiler and CHP system

As seen in figure 5.11 the Power-Unit is the centerpiece of the CHP-subsystem. Natural gas powers the piston engine, which works by the Otto cycle principle. The kinetic energy of rotation is transformed by the generator to electrical energy. Because of thermodynamic and construction-related limitations, over 70% of the used fuel energy is transferred to heat energy. In a closed cooling circuit most of this heat energy is passed to the Heat Distribution-Unit. Using a plate heat exchanger the

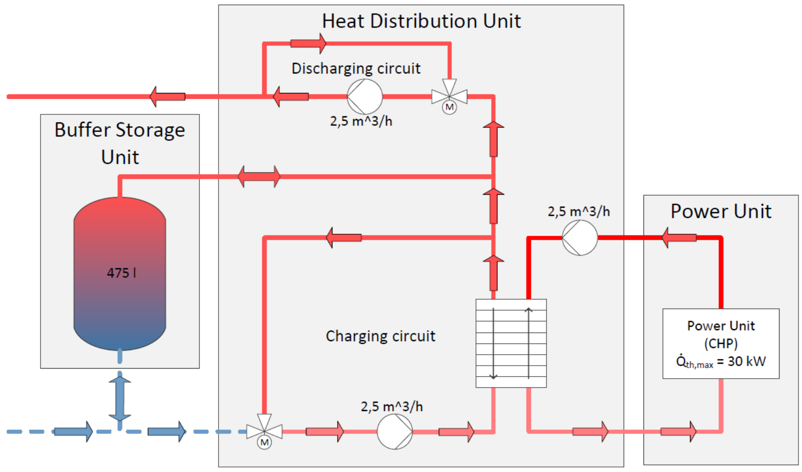

Figure 5.11: Combined Heat and Power Unit - overview

heat of the Power-Unit (heater fluid) is exchanged by the Heat Distribution-Unit to the high temperature circuit or directly to the Storage-Unit (heated fluid). Depending on the operation of the Power-Unit, the pump in the closed cooling circuit switches off or on. If switched on, it operates at a constant mass flow rate of 2.5 $\frac{m^3}{h}$.

The model for the CHP itself is a black box model and uses characteristic curves from the manufacturer to calculate the behavior of the real CHP. The heat storage tank model and the one for the heat distribution unit are similar to the ones used for the heat pump system.

In figure 5.12 the structure of the boiler-subsystem is shown. For each boiler a feedback of the flow line to the return line is implemented. The principle of the inner circuit is analogical to the charging and discharging circuit of the CHP-subsystem

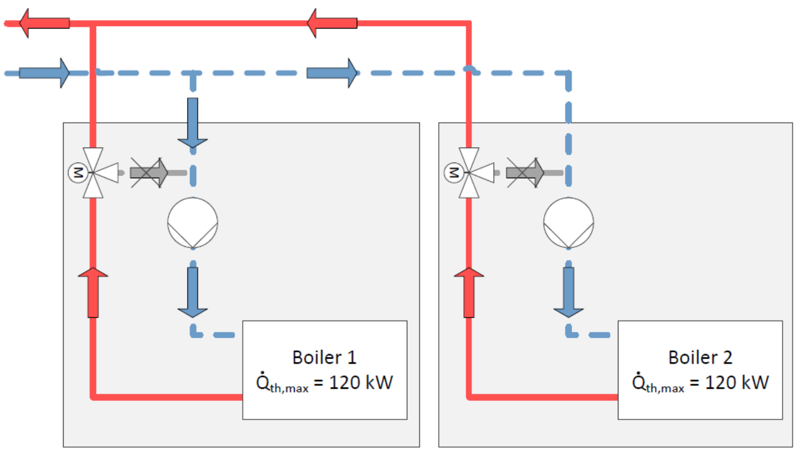

Figure 5.12: Boiler-subsystem - overview

The boiler model is a physical model, with a simplified firing system. Thermal mass of the boiler, minimal turn off time, table based dependency of efficiency from the load, set point hysteresis as well as a modulating interval for the power are part of the model.

The control strategy parts of the building automation system, required for the high temperature circuit, have been modeled in Simulink. The developed subsystems for Dymola have been simulated on their own using the monitoring data for all the required inputs. As the next step each subsystem has been simulated in combination with the Simulink model using BCVTB (BCVTB-SUB). Lastly, the high temperature circuit has been modeled, using the developed subsystems (BCVTB-HTC). Applying BCVTB, the high temperature circuit has been simulated in combination with the

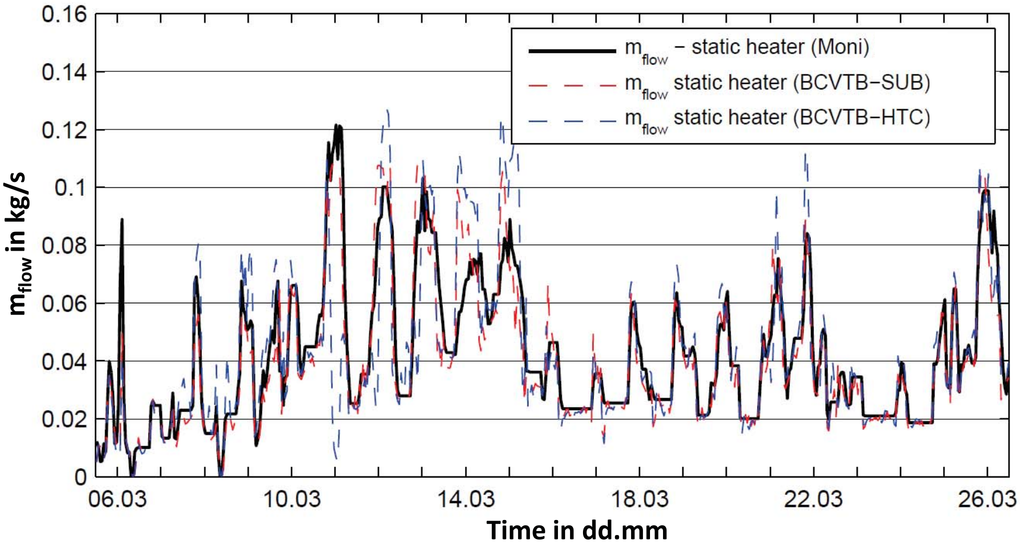

Figure 5.13: Comparison of measured data with simulated data for the mass flow rate

control strategy model and the physical inputs have been reduced to a minimum of boundary conditions of the high temperate circuit (heat demands and the connection to the low temperature circuit). Each subsystem in Dymola has been validated by comparing the results of both simulations using BCVTB to the monitoring data. Characteristic figures for the mass flow have been considered for the evaluation, as shown in figure 5.13. The simulation results of the consumer subsystems show good agreement with the monitoring data and can reproduce the current state of these subsystems. We consider the model to be a satisfactory.

5.2.3 Central air conditioning unit

Figure 5.14 presents the operation principle of the central air conditioning unit: the outside air is dehumidified in the absorber und then cooled down in the heat exchanger with the use of the return air, which in its turn was cooled down through a process of evaporative cooling.

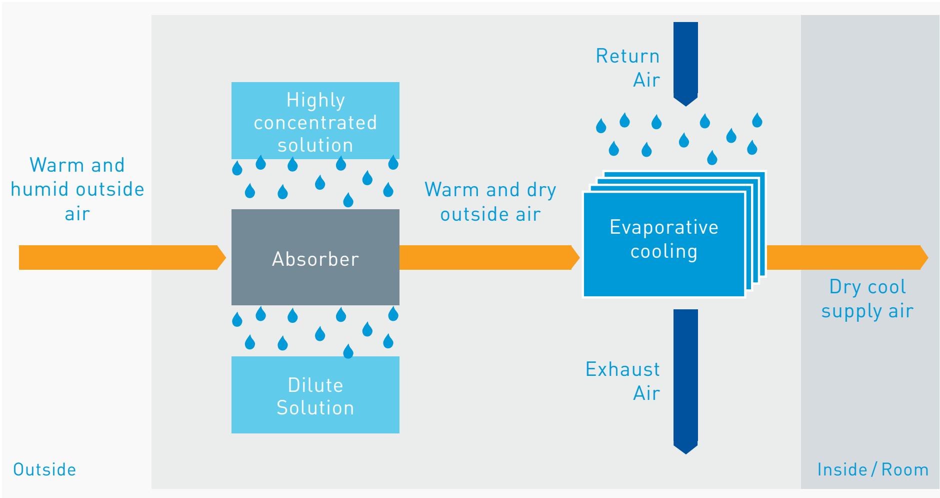

Figure 5.14: Cooling and humidification of the supply air [MenergaGmbH, 2009]

The evaporative cooling was done as a two-stage indirect adiabatic cooling. The model is straightforward using a heat recovery coefficient determined from experimental data and setting up energy and mass balance for the dry air and the water. The heat recovery coefficient depends on the volume flow of the return air.

The absorber unit was more difficult to model, as several design parameters have to be taken into consideration. The absorber is designed as a cross-flow exchanger to dehumidify the outside air with a brine solution. The contact area between the brine and the air is increased by filling the exchange volume of the absorber with Pall rings. The brine is sprayed form the top of the absorber on a packed bed of such rings. There are different geometrical forms possible for the Pall rings to distribute the liquid flow by sprinkling. The model build is specific to the central air conditioning unit installed in the building, as several used formulas are only applicable to this type of construction and Pall rings.

Modeling the absorbtion process requires a discretization of the volume of the absorber unit and setting up mass and energy balance equations for each discretization element. Figure 5.15 shows the two dimensional discretization principle used: when the values for the state variables for gas and fluid are known at the entry point in the absorber, the values at the exit of the absorber can be calculated, by step-by-step calculation through each cell. The model was further adapted to account for the drift induced by the air coming with a certain velocity into the chamber and influencing the flow of the sprayed brine.

Comparison of the simulation results was possible with measurement data done in a laboratory for this particular unit and made available as part of the final report for a project funded by the German Federal Ministry of Education and Research (funding code 032 9151 N). The relative errors for the achieved relative humidity, air temperature and brine concentration were under 6% over all

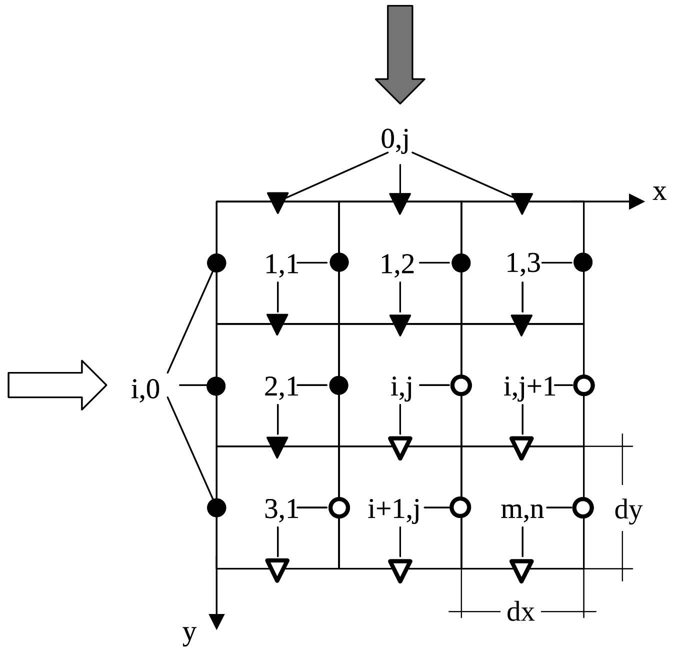

Figure 5.15: Principle of the 2D-discretization of the absorber volume [Elsenheimer, 2003]

simulated experiments. The model is considered satisfactory.

5.2.4 Geothermal field

For the geothermal field three models were built:

- one detailed model for a whole geothermal field with axial discretization of the borehole heat exchangers and spatial discretization of the ground
- one detailed model for a borehole heat exchanger with a radial ground model, which is a simplification of the first model
- one simplifed model for the whole geothermal field, used for long term analysis

Figure 5.16 shows the main components of a detailed model for a borehole heat exchanger, while presenting a discretization element. At the end towards the ground surface the pipes are connected to the neighboring pipes, at the other end they are connected to each other through a hydraulic resistance. The detailed model is used for short term analysis as depending on the dimensions of the geothermal field the required computational power can be quite high. A simulation for a geothermal field with eleven double u-boreholes, with four discretization elements for each pipe is the largest model built with this model.

The ground around the boreholes is discretized more finely near the boreholes, and more coarsely further away from them, in order to accurately model the energy storage into the ground through

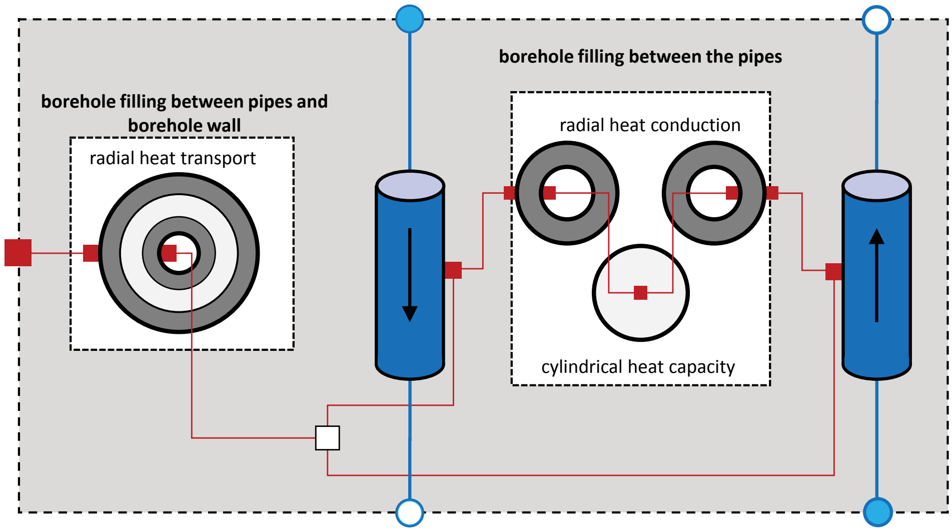

Figure 5.16: Detailed model of a borehole heat exchanger: one discretization element

dynamic loads: the temperature of the volume nearest to the boreholes reacts the quickest. Special care has to be taken with the initialization temperatures of the ground model, as depending on operation history, energy has already been stored into the geothermal field and will be extracted at a later point in time: e.g. storing heat during the summer and extracting it during winter. A good initialization temperature can be found by using measurement data and conducting a sensitivity analysis on the initialization temperature of the model.

Figure 5.17 shows the comparison between the simulated, $T_{RL,sim}$, and the measured return temperature, $T_{RL,mess}$ for the above mentioned field of eleven boreholes.The signal for the flow temperature, T_{VL} was taken from monitoring results. When building the relative error related to the temperature difference between flow and return temperatures we obtain a value of 19.5%. However these results were obtained after finding the best fit for the initialization temperature and using reliable values for the physical properties of all the materials involved: ground, borehole filling, pipe material and medium inside the pipes. The model is considered accurate enough, in the absence of better parameters.

The model built for long term analysis is based on the theory of g-functions as developed by Eskilson [Eskilson, 1987]. The g-functions are used to model the long term influence of the boreholes on each other depending on their position in the geothermal field. Figure 5.18 shows a possible clustering of the boreholes in the geothermal field around the main building. After doing the clustering, it is possible to analyze the way these four clusters influence each other over longer periods of time.

No comparison with measured data from the geothermal field was possible for this model, as the field had only been in operation for a short while.

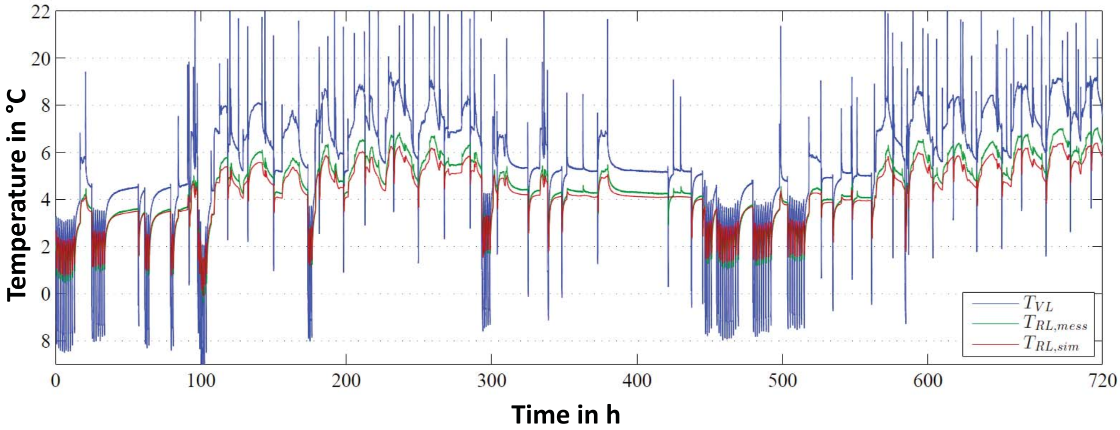

Figure 5.17: Comparison between the measured and the simulated return temperature for a geothermal field

5.2.5 Concrete core activation and façade ventilation units

The model for the concrete core activation is a physical model of a pipe running through the concrete layer of the wall. A discretization of the model leads to a connection of the pipe elements in series. As the concrete core activation model was part of the room model tested with measurements from the building, it is considered accurate enough.

The façade ventilation unit is a complex piece of technical equipment, as seen in figure 5.19. It has a heat recovery system with additional heat exchangers for cooling and heating of the supply air. If the air quality is adequate, but heating and cooling of the room is required, the unit can condition only circulating air, by opening the circulation valve. The heat recovery heat exchanger can be bypassed when the outside temperatures are too low, in order to prevent condensation. The model is a grey-box model, with black-box models for the heat exchangers and the ventilators. The tables for the black box models have been obtained by in-house measurements, so in this way the model is considered accurate enough.

5.3 Co-simulation aspects

Compared to experimental tests, simulations provide the important advantage of being able to test a considerable amount of different scenarios in a very short period of time. Furthermore the testing of extreme scenarios, as in the case of very high or very low outside temperatures, is possible. A further step in using the whole potential of the simulation is to connect simulation models between themselves, or to connect simulation models with real hardware (Hardware-in-the-Loop).

For the E.ON ERC main building we used co-simulation in three instances:

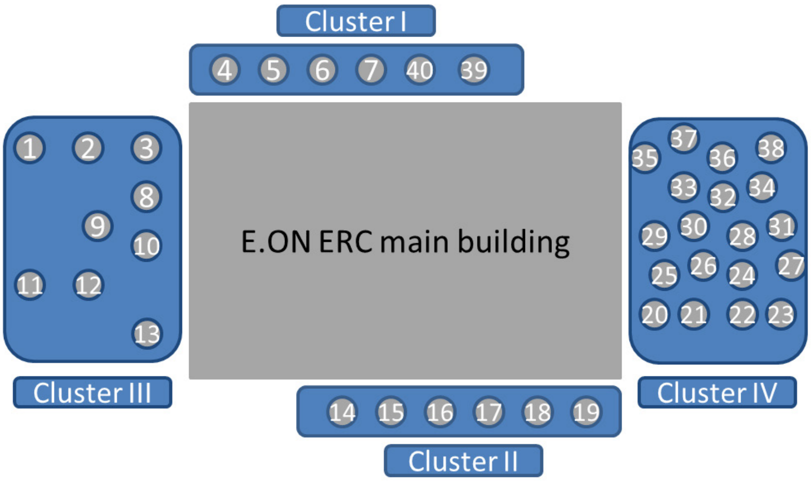

Figure 5.18: Clustering of the boreholes in the geothermal field of the E.ON ERC main building

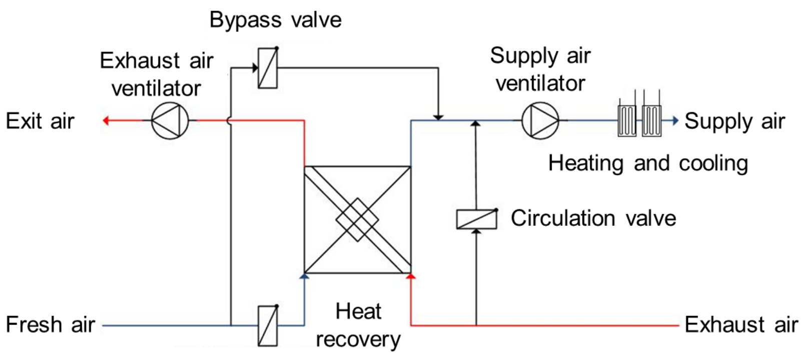

Figure 5.19: Diagram of façade ventilation unit

- for connecting a room model with the actual controller of the façade ventilation unit: co-simulation with C# interface
- for connecting several room models (tower concept) with an optimization algorithm written in MATLAB for the control strategy: co-simulation with BCVTB
- for connecting the model for the heat pump system or the CHP system with a control algorithm written in Simulink: co-simulation with BCVTB

5.3.1 Co-Simulation with C# interface

In order to be able to test modifications of the control strategy easily and fast, the simulation model is separated from the control strategy. Only the building and construction units are implemented in Modelica / Dymola. The control software remains its original proprietary software and on the original hardware of the façade ventilation unit. Thus the model and the controller have to communicate in set time steps. This type of simulation, although focusing only on the controller software is called Hardware-in-the-Loop, because the transmission of the signals inside the controller unit is done by the real piece of hardware.

The data from the controller includes: ventilator power, flaps positions, valve positions for the heating and cooling heat exchangers. This data is transmitted to the model as input parameters for the façade ventilation unit model. They lead to a new state of the room: new air temperature, new CO_2 levels, new relative humidity. The results of the simulation in return are send to the controller and used for new control decisions. In order to enable this communication, software in C# has been designed: routines for sending and receiving the information from the controller via HTTP-requests.

5.3.2 Co-Simulation with BCVTB

For connecting a control algorithm written in MATLAB with the simulation model we used BCVTB.

The MATLAB routine consists on one hand of the control algorithm, which calculates new temperature set points for the room models, by using a linear combination of the following factors: outside air temperature, wind speed, solar radiation, current room temperature and presence in the room. On the other hand an optimization algorithm is included which fine-tunes the parameters from the linear combination by using simulations of the following 48 hours incorporating weather and user behavior forecast data.

We used BCVTB for connecting each of the models of the heat pump system and of the CHP system with a control implemented in Simulink. We chose this approach as Simulink is easier to use and understand for building controllers than Modelica is. As the effort for optimizing the control strategies of these systems was done in a team, we chose a tool which would best aid the communication inside the team.

6 Results

The MCIS started gathering data from September 25th, 2012. Until March 2014 the system operates still not in a final mode according to its planning. Its energy efficiency is sub-optimal, since the system operates in maintenance, hand or back-up modes until end of February 2014. A final control strategy has been implemented in March 2014 and has to be tested and validated as a future task. Taking this into account, it has to be said, that all results presented in the following are not indicating the final system's efficiency. Nevertheless, we present the results of the MCIS in order to demonstrate the dimensions and the methodology of analyzing and visualizing the building's data.

The system has to be reevaluated when a final operation mode is implemented and under regular operation.

6.1 Monitoring results

Within the phase of taking the building into operation several studies have been conducted. Their outcomes served to develop the all new control strategy presented in chapter 3.2 and to validate the energy concept. Studies have been conducted towards the global energy demand, the energy conversion system, the energy distribution system, the energy use and thermal comfort, the electricity consumption and electric energy flows, the sorption-supported air handling units, and the concrete core activation system. Even thought all studies provided interesting results we present exemplary results for the global demand study and the energy conversion system study. The others studies and their outcomes are summarized. All detailed studies' reports are available upon request at our institute.

6.1.1 Global energy demand

Involved sensors in the global energy demand evaluation are, for consumed non-regenerative energy, gas counters and electricity meters. For regenerative energy, we use temperature sensors and flow sensors to calculate heat flows and here, regenerative energy transfer.

The global energy demand balance E_{global} of the building consists of electric energy E_{el}, chemical enthalpy within gas E_{gas}, and regenerative parts as energy exchange via geothermal field E_{GTF} and glycol cooler E_{GC}.

$$E_{\text{global}} = E_{\text{el}} + E_{\text{gas}} + E_{\text{GTF}} + E_{\text{GC}} \tag{6.1}$$

Electric energy and gas consumption represent the fossil energy demand, thus, the energy balance of non-regenerative energy is shown in equation 6.2.

$$E_{\text{global,non-regenerative}} = E_{\text{el}} + E_{\text{gas}} \tag{6.2}$$

Line and carpet plots are suitable to visualize the global energy demand.

The overall electric energy consumption for one year during the period from November 1$^{\text{st}}$, 2012 to November 1$^{\text{st}}$, 2013, is 705.84 MWh. This ends up in 98.57 kWh/m^{2}a with a floor space of 7161 m^2. These numbers may underestimate the real demand, since the heat pump did not operate continuously throughout the whole year. Furthermore, in May 2015, the building is in transition towards ordinary operation. Representative energy consumption data will be available after several years of such ordinary operation as already mentioned above. In order to show data processing and visualization concepts, we show results for one reference week starting 21.10.2012 until 27.10.2012.

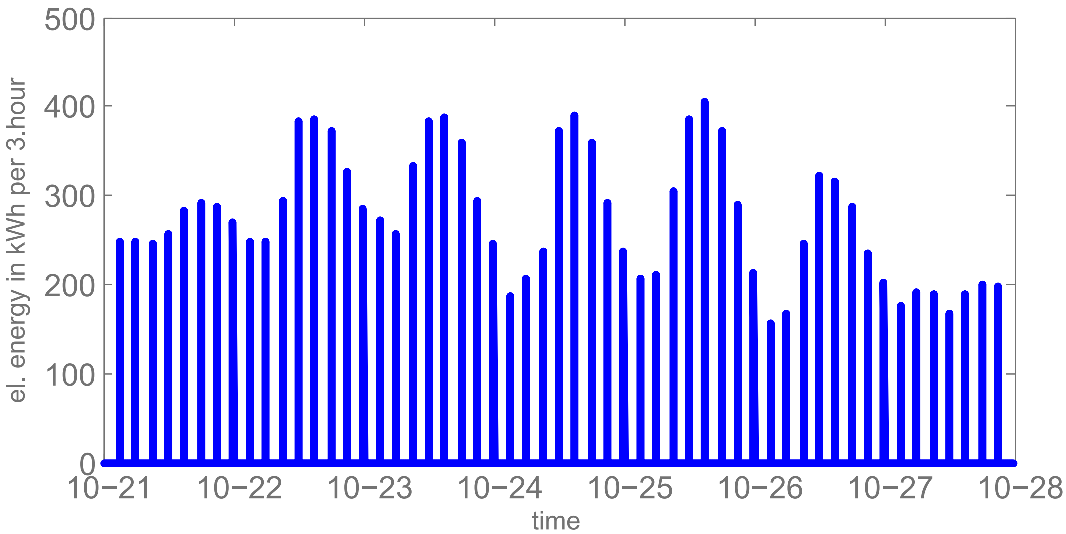

Figure 6.1: Consumption of electrical energy within reference week

Figure 6.1 shows the electric energy consumption for one week, clustered in three-hour-intervals. This reveals classical energy consumption schemes. The building consumes less energy during night times as during day times. Likewise, we can differentiate weekdays, with an average energy consumption of 2338.2 kWh, and weekends, with an average energy consumption of 1813.5 kWh. Offices are only occupied during weekdays. Accordingly, only computers for simulation purposes are operating, the light is switched off and household devices are not in use.

Less obvious results in terms of gas consumption shows figure 6.2. Gas consumption does not clearly correlate to ambient temperature. Still, it does correlate with day times. The building consumes more gas during day than during night. We can identify that on the days shown increasing gas consumption accompanies decreasing ambient temperatures. Due to the energy concept and its manifold ways of heat generation a correlation cannot be stated.

Absolute values of gas and electricity consumption are shown in table 6.1.

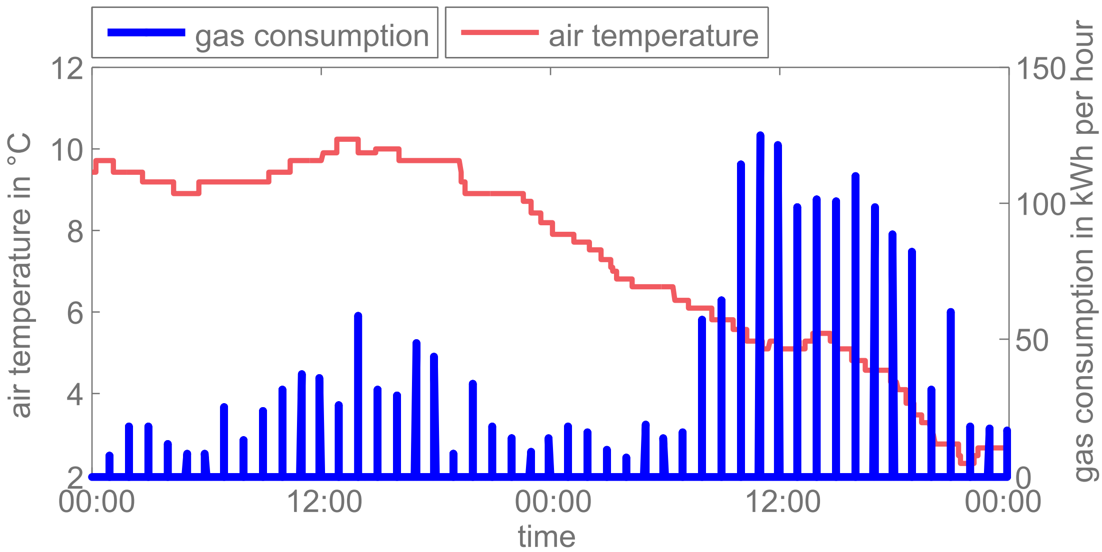

Figure 6.2: Gas consumption and ambient temperature for two day during reference week

Table 6.1: Reference week's electricity and gas consumption

	12/10/21	12/10/22	12/10/23	12/10/24	12/10/25	12/10/26	12/10/27
electricity in kWh	2126	2538	2530	2279	2384	1933	1501
gas in kWh	310.318	365.792	398.048	587.776	573.664	1402.195	601.888

Target indicators for annual energy consumption are annual electricity demand, specific annual electricity demand, annual gas consumption, and specific annual gas consumption. Having these numbers, we can calculate primary energy consumption and energy costs and, thus, compare the building to other buildings. These indicators form a base case for any energy related building optimization. As already said above, any calculation of these numbers would be misleading until the building does not operate in a final operation mode.

6.1.2 Energy conversion

A detailed analysis of the energy conversion system data, 70 days of Mai to July, took place during summer 2012. Involved systems have been the heat pump, the heat storage, the cold storage, the geothermal field, the glycol cooler, the condensing boiler system, the co-generation plant, and the main heat exchanger between high and low temperature heating grid. We used volume flows, temperatures, gas consumption and electrical power in order to calculate performance numbers and to visualize the operating behavior in diagrams.

We used two representative days to evaluate the performance of each system, a cold day and a warm day. Further, we analyzed the heat flows within the high and low temperature heating grids, the cooling grid and the energy dissipation system, i.e. geothermal field and glycol cooler.

This analysis succeeded in investigating the operational behavior of all energy conversion units. A MATLAB framework has been developed to further analyze any conversion unit at any time in future.

On the one hand, the study showed that the cooling system operates with high effectiveness. The system is able to fulfill the building's daily cooling demands. On the other hand, the study revealed weaknesses in operating performance of the system. The control strategy of the interaction between energy conversion units has to be optimized. More precisely, the optimization has to focus on the integration of the geothermal field and on the extension of heat pump's operation cycles length. Further, it should focus on the adjustment of volume flows around heat and cold storage.

Concerning the high and low temperature grids, the study revealed inefficiencies due to sub-optimal control. The analysis of the heat exchanger between these to grids showed, that the condensing boiler system produced large amounts of heat, which has been transferred to the low temperature grid, even though no heat generation would have been necessary. From an exergetic point of view and during the evaluated time period heat generation should have been accomplished via the heat pump.

The outcomes of this study have been integrated in the new control strategy, which has been implemented until March 2014. This control strategy is described in chapter 3.2.

In the following, we present only selected results as not all results can be shown due to the scope of this report. The whole analysis is available upon request at our institute.

Heat pump

As an exemplary result of the heat pump's analysis we present results from a cold summer day, June 19^{th}, 2012.

On that day, the heat pump is operated in cycles. It starts in average each 67.9 minutes and operates for 10.8 minutes. All together, it operates 21 times that day. Between 10:00 o'clock and 17:00 o'clock it operates in average each 63 minutes, whereas during the other hours only each 71.4 minutes. In that time a cycle is 12.8 minutes, whereas during the other hours it is only 9.9 minutes.

The temperatures and volume flows are shown in figure 6.3 respectively in figure 6.4. On the heat pump's hot side, inlet temperature, $\vartheta_{\mathrm{HP,h,in}}$, and outlet temperature, $\vartheta_{\mathrm{HP,h,out}}$, evolve between 34 and 35 °Cduring non-operation and between 37 and 38 °Cduring operation. A maximum of 39.5 °Cis reached. On the heat pumps cold side, inlet temperatures, $\vartheta_{\mathrm{HP,c,in}}$, and outlet temperature, $\vartheta_{\mathrm{HP,c,out}}$, vary due to the load status of the cold storage between 9.5 and 13.5 °C. On June 19$^{\mathrm{th}}$, 2012, on the heat pumps hot side, the volume flows, $\dot{V}_{\mathrm{HP,h}}$, are 15.8 l/s during downtime and 18.2 l/s during operation cycles. On the cold side a constant volume flow,$\dot{V}_{\mathrm{HP,c}}$, of 13.3 l/s is observed.

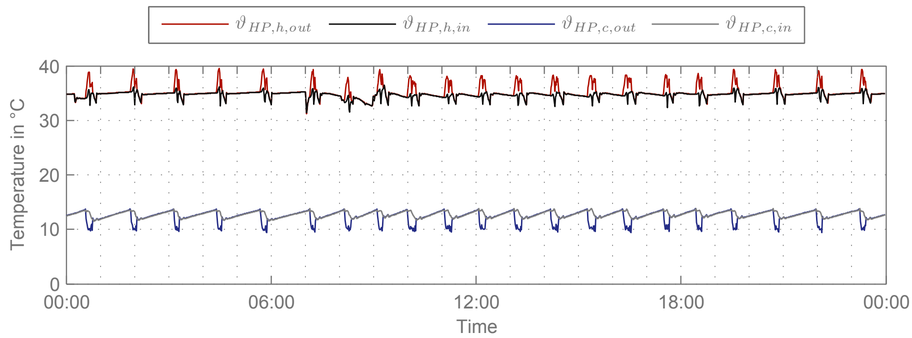

Figure 6.3: Heat pump's temperatures on June 19$^{\mathrm{th}}$, 2012

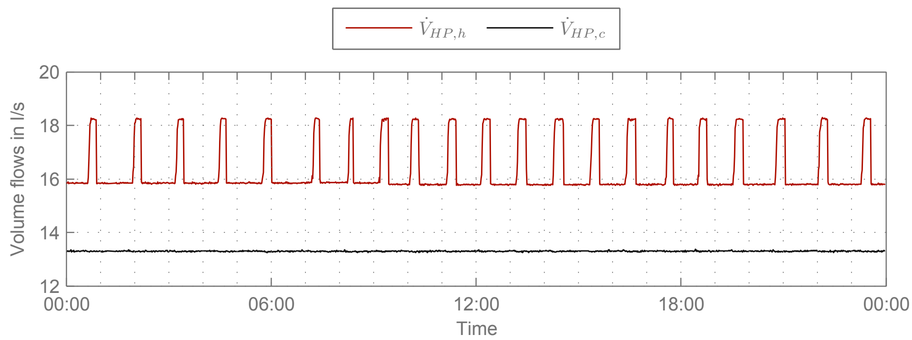

Figure 6.4: Heat pump's volume flows on June 19$^{\mathrm{th}}$, 2012

The heat pumps reaches at its hot side a thermal power output, $\dot{Q}_{\mathrm{HP,h,out}}$ of more than 200 kW. On June 19$^{\mathrm{th}}$,2012, the maximum value is 306 kW, as figure 6.5 shows. On its cold side it averagely operates with a thermal power, $\dot{Q}_{\mathrm{HP,c,in}}$, between 150 and 160 kW. A peak of 194 kW is measured. During downtime a heat flow of 10 kW is constantly recorded. The values above give an equivalent average power of 152.9 kW on the cold side and 198.2 kW on the hot side.

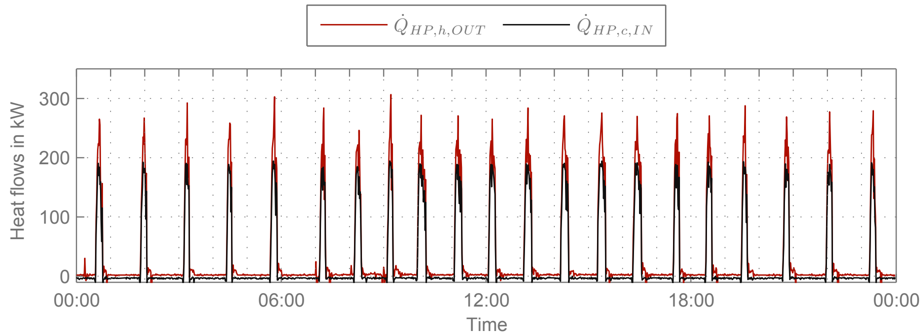

Figure 6.5: Heat pump's heat flows on June 19th, 2012

On June 19th, 2012, the heat pump transferred an amount of 507.9 kWh thermal energy, $Q_{\mathrm{HP,c,IN,total}}$ to a higher temperature level, generating 796.0 kWh thermal energy $Q_{\mathrm{HP,h,out,total}}$. Further, figure 6.6 shows inlet, $Q_{\mathrm{HP,c,IN,run}}$, and oulet,$Q_{\mathrm{HP,c,IN,run}}$, energies per cycle. As it can be seen these energy amounts vary.

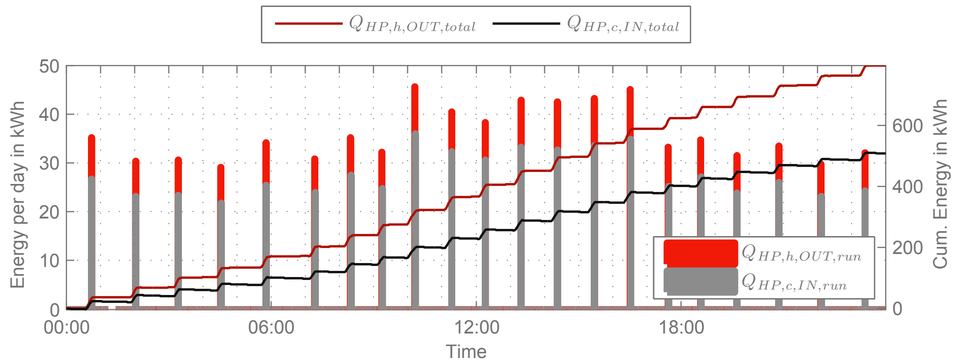

Figure 6.6: Heat pump's energy per operating cycle and cumulated energy on June 19th, 2012

For June 19th, 2012, a cooling energy efficiency ratio of 3.38 is calculated.

Geothermal field

As further exemplary result we show the analysis of the geothermal field for June 19th, 2012, in the following.

The field shows a cyclic operation behavior comparable to the heat pumps behavior. Most of the time, energy from the building is transferred to the field. This heat transfer direction alternates periodically, meaning heat is transferred from the field to the building. This process is repeated with nearly the same frequency as the cyclic operation behavior of the heat pump.

Figure 6.7 shows inlet temperature, $\vartheta_{\mathrm{GTF,in}}$, outlet temperature, $\vartheta_{\mathrm{GTF,out}}$, and volume flow, $\dot{V}_{\mathrm{GTF}}$

for the geothermal field. The volume flow shows variations between 0.5 l/s and 1.5 l/s. At each operation cycle a peak of 8 l/s is measured.

The field's outlet temperature remains with 12.4 to 12.5 °C quite constant, independent of the heat pump's operation cycles, whereas the inlet temperature varies between 14.5 and 16.3 °C.

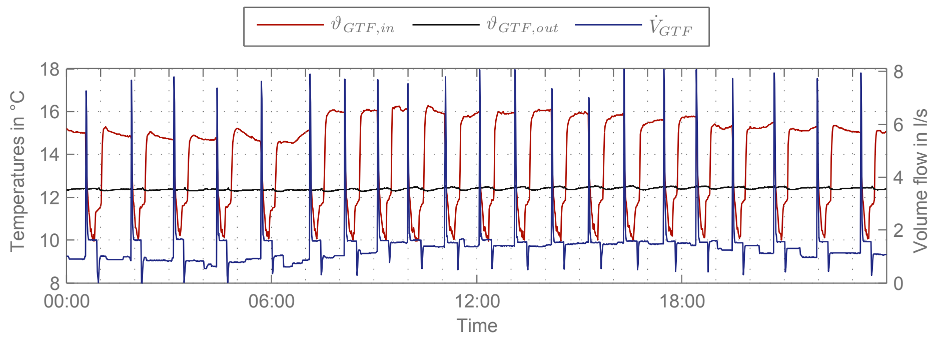

Figure 6.7: Geothermal field's temperatures and volume flow on June 19th, 2012

The field's thermal power output, $\dot{Q}_{\mathrm{GTF,IN}}$ evolves throughout the day between −16 kW and 25 kW. Figure 6.8 shows further the energy, $Q_{\mathrm{GTF,IN}}$, transferred to the field. At the end of the day it rises up to 192 kWh.

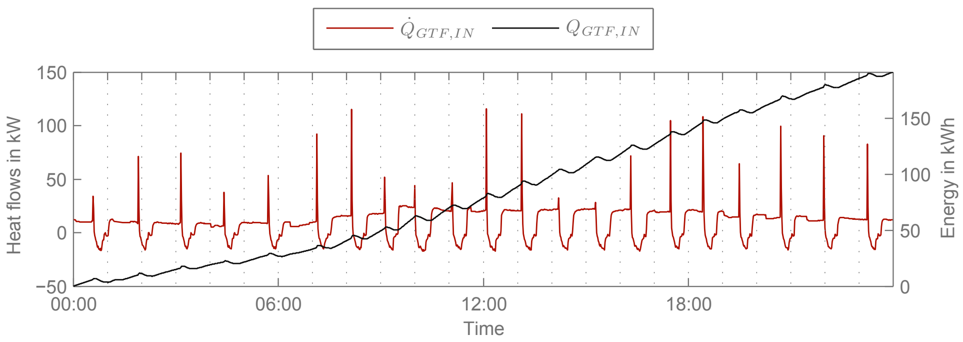

Figure 6.8: Geothermal field's heat flows and energy on June 19th, 2012

Overview energy flows

All above presented results are integrated to different diagrams and overview chats. As an example, in figure 6.9 we present the overview diagram of the daily energy flows on June, 19th, 2012. It integrates all results above and of other energy conversion units analyses. Via this figure, the energy flows within the building and the interaction of energy conversion units become visualized.

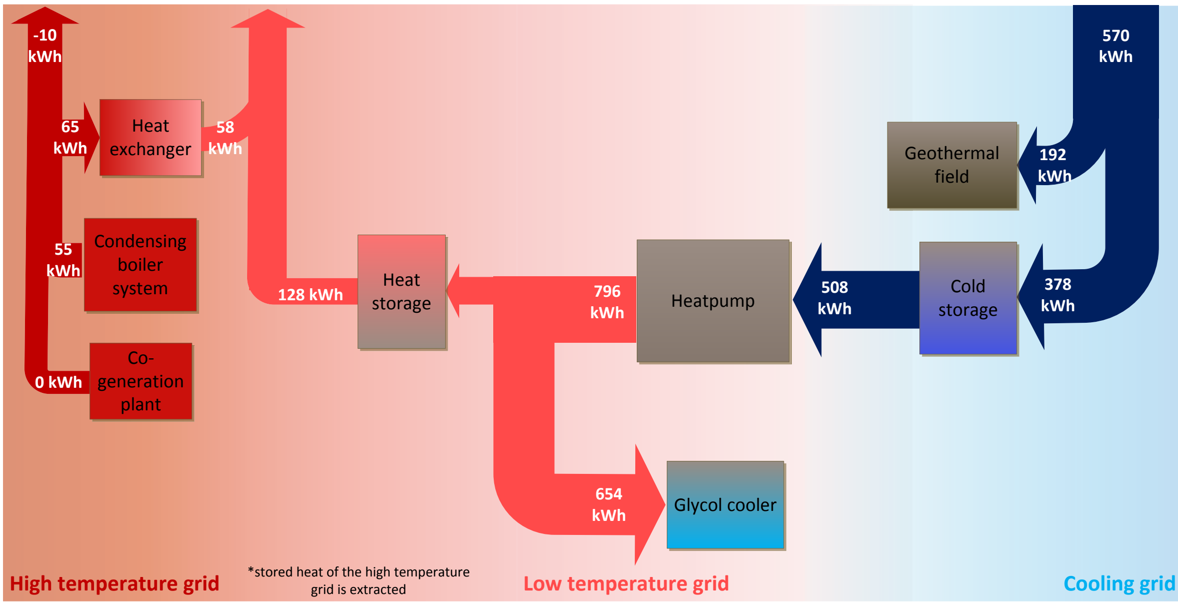

Figure 6.9: Overview energy flows in high temperature, low temperature and cooling grid on June 19th, 2012 (hot day)

6.1.3 Energy distribution

A complete analysis of the cooling and heating energy distribution system has been conducted. As the building has a multifunctional character it possesses different zones and usages. Thus, we face different, unpredictable and varying energy demands which have been analyzed within this study. The study focuses on concrete core activation and façade ventilation units. Specific performance numbers have been calculated for these two systems. The study can be repeated at any time to any given period thanks to a developed Python framework.

The main results of this study have been that the concrete core activation is only used for cooling purposes when the ambient temperature lies above 22.5 °Cand that too much cooling energy has been provided via façade ventilation units. Façade ventilation units have even been cooling against the heating of the concrete core activation. As described in chapter 3 the concrete core activation should be a base load system, supported by the more dynamic system of façade ventilation units. The control strategy concerning the interplay between concrete core activation and façade ventilation units has to be adjusted and optimized as a future task.

Further, the study revealed that façade ventilation units operate until 23:00 h, even though normal working times are then already over. Even further, a peak in cooling engery from façade ventilation units occurs daily between 23:00 h and 00:00 h. Thus, the control strategy of the façade ventilation units has been adjusted, covering these two facts.

Whether the concrete core activation's design is sufficient or not has not been evaluated to final extent. This has to be done in a future task.

6.1.4 Energy usage and thermal comfort

Within this study, a combined evaluation of thermal comfort and energy flows within different representative office rooms has been conducted.

For thermal comfort, Fanger's predicted mean vote (PMV) and percentage of people dissatisfied (PPD) have been used. The results show that 95 % of measured values have been within category B, following DIN EN ISO 7730, during the evaluation period between August 7th and 16th 2012[1]. This means that a high level of thermal comfort is reached within office rooms of the E.ON ERC main building.

The study revealed, according to the study presented in chapter 6.1.3, that, also on room level, heating and cooling takes place at the same time. It reinforces the need for an optimization of the control regime between concrete core activation and façade ventilation units. Further, it calculates the maximal daily cooling energy within the evaluation period with 497 Wh/m^2 on room level.

The indoor air quality, evaluated in parts per million volatile organic compounds (ppm VOC) and CO_2, has been very good throughout all inspected rooms. Thus, the ventilation via decentralized façade ventilation units is effective. The maximum measured concentration of CO_2 has been 592 ppm and is thus far below the suggested limit of 1000 ppm.

6.1.5 Electricity

This study focused on implementing an electric energy monitoring system within the E.ON ERC main building. During the construction of the building energy meters have been installed following the plans from the planning engineers. Within the Energy Concept project, so-called M-BUS masters have been installed. Communication problems occurred that could not have been solved, due to limited time and resources. In Mai 2014, the electric energy monitoring is still incomplete. It has to be taken into operation as a further task. Further, more sensors have to be installed, as it was implemented during the building's construction phase according to external plans, the sensor placement is not suitable for drawing a complete picture of energy flows within the building.

The outcomes of the studies are the global electric energy demand and a concept for a complete electric monitoring system, that has to be implemented within a further task.

The building consumes a peak power of 220 kW. The base load is between 50 kW and 80 kW. The mid load lies between 80 kW and 110 kW. The heat pump is identified as the main electric energy consumer. The yearly specific electric energy consumption is interpolated to round about 90 kWh/m^2a.

[1] All assumptions and parameters are described within the detailed study, available at our institute upon request.

6.1.6 Sorption-supported air handling units

We developed and implemented a monitoring system for the sorption-supported air handling units. The developed system enables to visualize all energy flows and state within one of the sorption-supported air handling units. Further a data evaluation concept has been developed, deriving efficiencies numbers and performance indicators for each component within the air handling units.

A major challenge has been the measuring of air volume flows. We installed eight further temperature and humidity sensors, able to calculate via energy and mass balances the volume flows at all stages of the air handling units. The developed and implemented data processing framework can be reused at any time for further evaluations and assessments.

The system evaluation showed, that the heat recuperation is well implemented and the internal control strategy of the units is working well. The external control strategy, thus the integration into the building showed weaknesses and has been improved. Further improvement is necessary towards the integration of the evaporators, since desired humidity levels have not been reached.

6.2 Simulation results

In this chapter several activities are presented in which the control strategy for various components of the energy system were improved using simulation models. For each such activity the scope is firstly presented, then the used models and finally the achieved results.

6.2.1 Control development for façade ventilation unit

The façade ventilation units installed in the building are in themselves prototype. They provide a suitable system for testing new control strategies. On the one hand, these units are designed for decentralized operation and are therefore able to run independently from any building components. On the other hand, users can communicate directly with these units, via user interfaces. This communication can be monitored and as such the quality of the control strategy can be estimated.

We used a Hardware-in-the-Loop approach to test and improve their control strategy. Using this method, it is not necessary to transfer the control strategy into the code of a simulation tool, rather the existing controller is coupled directly to a building simulation model. This simulation model contains a thermal model of the façade ventilation unit, a room model and a weather model. The controller of the façade ventilation unit communicates the values of the control parameters to the simulation model. The simulation model runs a short simulation and returns the relevant room data to the controller, e.g. room temperature or CO_2-concentration. Based on these data, the controller is able to take a new control decisions.

Façade ventilation systems have to be able to deal with different characteristics for every single room equipped with such a module. The façade ventilation units are used in offices, which are different from one another through their orientation and their internal gains. However there has to be a single control strategy, able to provide optimal conditions for every single room at any time of the year. A very important task is to find fitting parameters for the internal PID-controllers of the heating and cooling supply. These controllers have to ensure fast adaptions of the room temperature according to the users' needs. On the other hand, oscillations of any actor, e.g. heating valve or ventilation fans, have to be avoided. The different controllers integrated in every actor of the façade ventilation modules are designed as PID-controllers. They are independent from each other, e.g. heating performance and ventilation power can be adjusted separately.

The tuning of the control parameters (proportional gain (Kp), integration time (TN), derivative time (TV)) is done by analyzing the behavior of the different actors with the initial controlling parameters. In order to learn about the behavior of the system, the controller is set up initially as a pure P-Controller (Kp=20, TN=0 s, TV=0 s). The tuning of the control parameters is done according to [Åström and Hägglund, 1995].

With the initial parameters a winter day (figure 6.10), as well a a summer have been simulated.

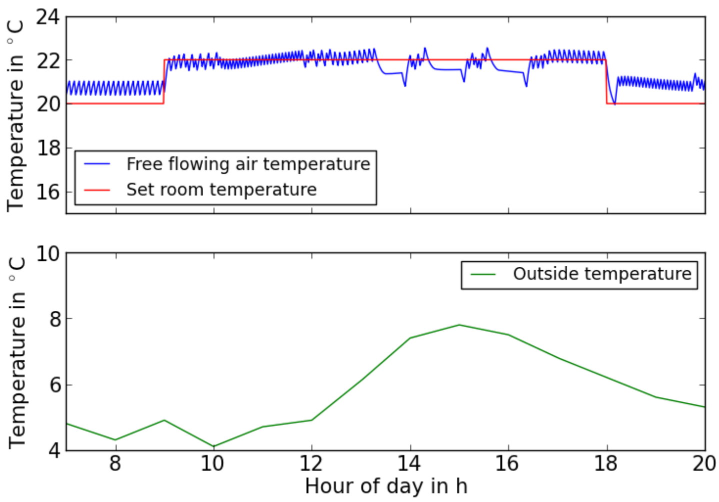

Figure 6.10: Room temperature at winter day with initial P-controller

After an iterative process the final parameters for the controllers were set. Figures 6.11 and 6.12 show the climatization performance of a winter day and a summer day after the tuning of the controller.

Regarding the winter day, it can be observed, that the controller leads to zero oscillations. During office hours (9:00 to 18:00), the temperature set point is approached very quickly and the room temperature is kept stable within a small range (set point ± 0.5 K) for the whole day.

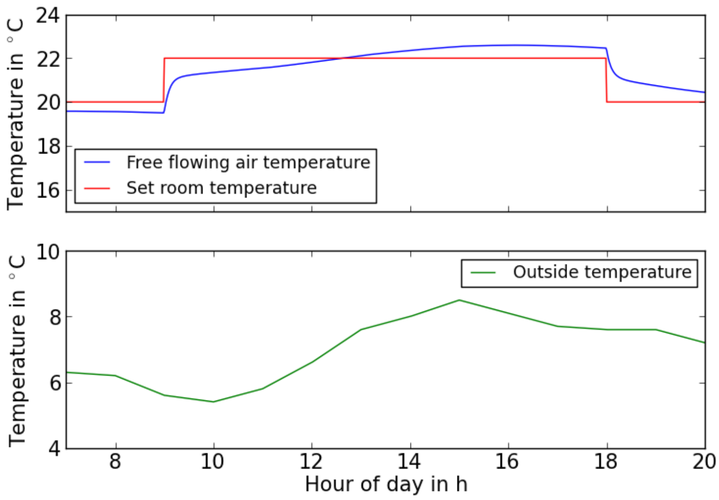

Figure 6.11: Room temperature on a winter day after tuning of controller

The simulation of a summer day shows good performance. The set point is reached after a short rise of the temperature.After reaching the set point, the value is kept stable. When the user is absent, deviations of 2 K are accepted. The control parameters assume to be applicable for heating as well as for cooling performance.

A future possible continuation of this work can focus on whether it is possible to use the Hardware-in-the-Loop method for controllers with automatic tuning as well as automatic design of complete controlling structures.

6.2.2 Control optimization for the heat pump system

The work done under this scope focused on improving the control strategy of the heat pump system, which was not able to cover the heat demand because of its sub optimal control strategy. The purpose was to develop optimization actions using a dynamic simulation, which would enable the real system to provide all the needed heat demand by the heat pump.

First a detailed analysis of the system was conducted to show the main malfunctions and their causes. The main causes of the deficient control strategy were identified as: the support of the heat exchanger, the behavior of the heat storage and the suction of its own feed flow by the heat pump.

According to the system analysis, a dynamic simulation model was developed, which shows the characteristic behavior of the real heat pump system. A comparison between real measured data and simulation results allows the validation of the model, as presented in chapter 5.

Three reference weeks with different heat demand profile were derived from measurement data

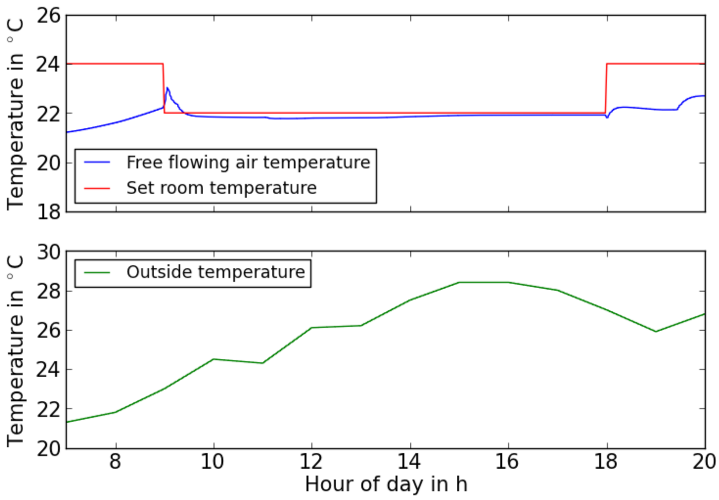

Figure 6.12: Room temperature on a summer day after tuning of controller

and used as test scenarios:

- a *cold* week, with distinctive heating-up periods at the beginning of each day
- a *moderate* week, where the difference between night and day mode became lower than in the former case
- a *transtion* week from heating to cooling mode

The optimization actions were evaluated using the following key performance indicators

- coverage ratio: the ratio between the energy supplied by the heat pump and the total energy supplied to the building
- hours of operation ratio: the number of operation hours of the heat pump divided by the duration in hours of the considered time interval
- cycle length: the number of operation hours of the heat pump divided by the number of on/off cycles

They were calculated for each experiment and compared to the reference state.

First of all, the run without support by the heat exchanger combined with the modification to a pressureless distributor was simulated. This leads to an increase in the *coverage ratio*, depending on the scenario, from 16% to 60% up to 100%.

As further optimization step, a return temperature control was implemented in the consumer circuit and a demand-actuated, idealized control of the volume flow was designed. The simulation results show an additional increase in *cycle length* from 8 min to 23 min up to 10 min to 32 min.

Finally, the optimization suggestion was given to run the real system without the heat exchanger and to transform the hydraulic distribution system to an pressureless one.

6.2.3 Exemplary results of PEBBLE project

The infrastructure of the building allowed for the demonstration of an ambitious European project called *Positive Energy Buildings through Better controL dEcisions* (PEBBLE, contract #248537) . The goal of the project was to reduce the energy consumption of the building under a comfort constraint of 15 % PPD. We demonstrated the project on the concrete core activation zone north of the building. The control algorithm was controlling the set points for the temperatures in the rooms and the flow temperature of the concrete core activation.

We ran offline as well as online experiments for the building. Offline experiments are experiments where no control parameters are sent to the building. Instead standard weather data and occupancy profiles are used. For the occupancy profiles we assumed continuous occupation according to the room book, between 9 a.m. and 6 p.m. The machines are on when the users are in the building, and go on standby during the night. The tower models were used in this approach.

The purpose of the offline experiments was to assess how fast the simulation runs and how good it works for all three towers. Summer and winter tests were done. For each test a period of two days was simulated, producing one set of controllers. To produce a set of controllers for one tower takes around 2.5 hours. Offline experiments meant to show the theoretical energy saving potential of the building offered promising results, of energy savings up to 75% in some cases in summer and 17% in winter, even when compared to very good rule-based controllers (temperature setback for night mode, set temperatures depending on the ambient temperature).

The real innovations of the new control algorithm when compared to rule-based controllers is the consideration of the indoor comfort, along with the dependence of set temperatures on more than just the ambient temperature.

Online experiments are the experiments where data is exchanged between the co-simulation and the building (figure 6.13). Controllers are developed and deployed continuously. They are developed with the help of a two day simulation but will only be used for three to four hours real time, during which a new controller is generated with improved prediction data for the near future. The simulation uses weather prediction data (updated hourly) and occupancy profiles. The occupancy profiles are similar to the ones used for offline simulations, but are further adapted to take into consideration the weekends.

The initial state of the simulation has to be the current state of the building, especially when dealing with the thermal mass of the concrete activated ceiling. To this effect, a *warm up* of the model occurs before each new set of controllers is determined. Monitoring data for the last 72 hours is used: room air temperatures, ambient conditions, presence, and flow temperature of the concrete core activation. The optimization then runs like in an offline experiment.

A problem of the offline experiments is the evaluation. Only six offices in the building are reference rooms, where the energy consumption of the concrete core activation and the façade ventilation

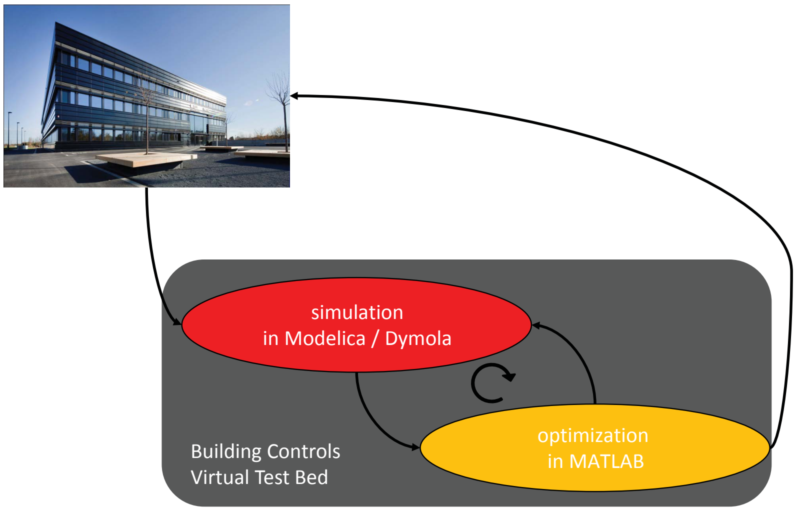

Figure 6.13: Data exchange flows during online simulations

unit can be measured. No two such rooms on the same floor have the same orientation. The occupancy profiles and the indoor comfort preferences of the people working in the offices are different.

Figures 4.14 and 4.15 presented exemplary results for evaluation efforts. It can be observed that the new control algorithms does change the set point temperatures quite dynamically, mainly according to indoor temperature, user presence and solar radiation. However this temperature cannot always be reached. The reason for this behavior may be a function of user involvement, e.g. opening the window, which leads to a shut down of the façade ventilation unit or a technical problem which prohibits the façade ventilation unit from functioning correctly. However the new control strategy adapts dynamically to the current conditions, implying better comfort values and does not seem to lead to higher energy consumption.

7 Conclusion and research prospect

Within this project, we developed an energy concept for the new E.ON ERC main building. During the building's construction phase, we assisted the implementation of the energy concept and implemented an user-added monitoring system. Together with a virtual server infrastructure, different data bases, data processing algorithms, and interfaces, this system became the monitoring, control and interface system (MCIS) which transformed the building into a control research demonstration bench.

Enabled by the extensive data available, we were able to build and validate several simulation models for the building and technical equipment. These models were than used to set-up and run test scenarios for the development and improvement of control strategies for different parts of the energy concept.

Monitoring data analyses and simulation studies enabled extensive system assessment and optimization via gathered knowledge and system insights. The optimization's result has been an all new control strategy, which we implemented during February 2014.

An online monitoring and data visualization system will publish daily, weekly, monthly and yearly building reports, integrated into the new E.ON ERC homepage. Further, a promotional display in the building's reception area informs about actual data points.

7.1 Conclusion

The implemented energy concept is able to fulfill all energy demands. Thermal comfort within the new building is more than acceptable.

From a control point of view, the project revealed serious defects which led to a high energy consumption. Thus, we developed a new control strategy which is now in its taking-into-operation phase.

The MCIS is in full operation and provides highly resolved monitoring data. Several following projects are enabled by the MCIS and are already taking advantage of the system.

With the help of the developed data processing framework it is possible to flexibly conduct assessments towards the energy conversion system, the energy distribution system, the energy usage, and the thermal comfort.

The developed thermal simulation models for the building with different degrees of detail, as well as the developed models for the technical equipment can be used in further research projects. An important lesson learned from this project is the difficulty of building up a detailed simulation model for the whole building with the complete model of the energy system as such a model is highly complex and thus very slow.

All the stages of the developed method for simulation-based testing and improvement of control strategies are documented in this report: building up simulation models, validation and improvement using measurement data, simulation-based testing and improvement of the control strategy, implementation into real building, and re-evaluation.

7.2 Research prospects

Since the project is limited in time and resources, there are tasks that have to be finished within future projects. One should validate the newly implemented control strategy and compute meaningful energy performance indicators for the system. The developed data processing framework will support this task. The interfaces in the system make possible to adjust set points from an external control development bed. Nevertheless, we need to enhance these interfaces towards the ability to control also system parameters, e.g. valve positions, dampers etc. The data processing and reporting system is working but needs maintenance to handle sensor defects and future work in terms of data filtering and failure robustness. An extension of the reporting system towards more diagrams and numbers will enhance the building's performance evaluation.

The project provides an ideal basis for future research projects. It will be interesting to implement an optimal control or fuzzy control regime and replace the rule-based control regime. The system can serve as a demonstration bench for agent-based control projects and, as already, for model-predictive control projects.

With the data available, we could design and validate more sophisticated simulation models. Further, the extensive data provides the possibility to derive user profiles, internal load coefficients, and reference energy performance data.

8 Literature

DIN EN ISO 7726: Ergonomics of the thermal environment - Instruments for measuring physical quantities, April 2002.

EnEV2009: Verordnung über energiesparenden Wärmeschutz und energiesparende Anlagentechnik bei Gebäuden, 2009.

VDI 2078: Berechnung der Kühllast und Raumtemperaturen von Räumen und Gebäuden, Mar 2012.

ASHRAE 140. Standard Method of Test for the Evaluation of Building Energy Analysis Computer Programs, 2007.

Karl J. Åström and Tore Hägglund. *PID Controllers: Theory, Design and Tuning.* Isa, 2nd edition edition, 1995.

Ana Constantin, Johannes Fuetterer, Rita Streblow, Dirk Mueller, Giorgos Kontes, and Dimitrios Rovas. Simulation assisted implementation of a model based control parameter fine-tuning methodology for a nonresidential building with a complex energy system. In *Proceedings of BS2013 : 13th Conference of International Building Performance Simulation Association, Chambéry, France, August 26-28*, 2013.

Dassault Systems. Dymola - multi-engineering modelling and simulation. http://www.3ds.com/products/catia/portfolio/dymola, 2011.

DIN V 18599. Energetische Bewertung von Gebäuden Berechnung des Nutz-, End- und Primärenergiebedarfs für Heizung, Kühlung, Lüftung, Trinkwarmwasser und Beleuchtung, Juli 2005.

Beckmann Duffie, John A. *Solar Engeneering of thermal processes.* Wiley, 2006.

F. Elsenheimer. *Energetische und exergetische Analyse unterschiedlicher Regelungsstrategien mit Hilfe von Simulationsrechnungen und deren messtechnische Validierung bei der sorptionsgestützten Klimatisierung auf Basis wässriger Lösungen.* PhD thesis, Universität Duisburg-Essen, 2003.

P. Eskilson. *Thermal analysis of heat extraction boreholes.* PhD thesis, Lund University, Schweden, 1987.

S. Baldi et al. A “plug-n-play” computationally efficient approach for control design of large-scale nonlinear systems. In *IEEE Conference on Decision and Control 2013*, Italy, 2013.

P.O. Fanger. *Thermal comfort.* Danish Technical Press, 1970.

M. Lauster, J. Teichmann, M. Fuchs, R. Streblow, and D. Mueller. Low order thermal network models for dynamic simulations of buildings on city district scale. *Building and Environment*, 73(0): 223 – 231, 2014. ISSN 0360-1323. doi: http://dx.doi.org/10.1016/j.buildenv.2013.12.016. URL `http://www.sciencedirect.com/science/article/pii/S0360132313003727`.

Markus Lichtmeß. *Vereinfachungen für die energetische Bewertung von Gebäuden.* PhD thesis, Bergische Universität Wuppertal, Fachbereich D - Architektur, Lehrgebiet Bauphysik und Technische Gebäudeausrüstung, 2010.

A. Maas, G. Hauser, and K. Hoettges. Energieeinsparverordnung. *Bauphysik*, 24, 2002.

MathWorks. *MATLAB and Simulink.* Massachusetts, USA, 2012.

MenergaGmbH. Ventilation and air conditioning technology sorption-supported air conditioning, 2009.

Modelica Association. Modelica and modelica association. Available: http://www.modelica.org [Online], 05 2011.

D. Müller and A. Badakhshani. Gekoppelte Gebäude- und Anlagensimulation mit Modelica. In *Proc. of BauSim Conference, Wien, Austria.*, Wien, September 2010. Proc. of BauSim Conference.

Michael Wetter. Modelica-based modelling and simulation to support research and development in building energy and control systems. *Journal of Building Performance Simulation*, 2(2):143–161, 2009. ISSN 1940-1493. doi: 10.1080/19401490902818259.

Henryk Wolisz, Ana Constantin, Rita Streblow, and Dirk Mueller. Performance assessment of heat distribution systems for sensible heat storage in building thermal mass. In *Proceedings of CISBAT 2013, 4-6 September 2013, EPFL, Lausanne, Switzerland*, 2013.

9 Attachments

9.1 Documentation of the user added monitoring system

The documentation of the monitoring System consists of various forms of information e.g. wiki entries, diagrams and text explanations. One part is a database in form of an excel-file where all of the connections between the expansion units, the modules and the items (sensors) are brought together and displayed as a pivot table.
The advantage of a pivot table is that you can search in both directions which means you can start from each expansion unit and display the entire way till an item or you can choose an item and then identify the module/expansion unit to which it belongs. Thus it does not depend on what information you have when you are searching for something.
Additionally, to the connection e.g. between an item and a module you can find the location of an item or an expansion unit in the building which is useful for the orientation in the building if it becomes necessary to repair or to change a broken sensor.
Another important part is the syntax of the item names. It is divided up into abbreviations for the locations and the functions of the items.
The aforesaid information belong rather to the hardware documentation part. The other part is kind of a software documentation and description of the functions and relations between the various hardware components.
There is therefore a wiki where you can find a tutorial e.g. to read out some data from the database and display it either with MATLAB or Microsoft Excel. In addition to the tutorials there are explanations of how the whole monitoring system works in general and explanations of how the modules, items and expansion units work in particular.
All in all, the idea is to have a documentation which is easy to handle for new people so they can start to work with the monitoring as fast as possible. It has to be expandable by everyone who uses it so the work of the administration of the documentation is not connected to only one person. Additionally, what is important for documentations are straightforward diagrams which are simple and which show the direct connections between the items and e.g. modules.
All of these points are fulfilled in the documentation of the monitoring system.

9.2 List of figures

9.3 List of tables

9.4 Publications

- Fütterer, Johannes; Constantin, Ana; Müller, Dirk. "An energy concept for multifunctional buildings with geothermal energy and photovoltaic". CISBAT 2011 : cleantech for sustainable buildings ; from nano to urban scale ; proceedings ; 14-16 September 2011, EPFL, Lausanne, Switzerland.
- Huber, Max; Constantin, Ana; Müller, Dirk. "Optimierung der Regelungsstrategie für ein Fassadenlüftungsgerät mit Hilfe von Simulation". Deutsche Kälte-Klima-Tagung 2011, Aachen, 16. - 18. November 2011 / DKV, Deutscher Kälte- und Klimatechnischer Verein.
- Huber, Max; Constantin, Ana; Müller, Dirk. "Software-in-the-loop method for optimizing the control strategy of a façade ventilation unit". Xe conference internationale sur la ventilation industrielle = 10th International Conference on Industrial Ventilation ; Paris, 2012, 17/18/19 Sept. / organised by the Institut National de Recherche et de Sécurité (INRS).
- Fütterer, Johannes; Constantin, Ana; Streblow, Rita. "Concept and Energy Management in the new E.ON ERC Main Building". Proceedings of the International Symposium in Sustainable Energy in Buildings and Urban Areas : 14 - 20 October, 2012, Kusadasi, Turkey.
- Fütterer, Johannes; Constantin, Ana; Schmidt, Martin; Streblow, Rita; Müller, Dirk. "Monitoring technique, evaluation methodology and results for a multifunctional building with

geothermal energy". Proceedings of CISBAT 2013 International Conference, 4-6 September 2013, EPFL, Lausanne, Switzerland

- Fütterer, Johannes; Constantin, Ana; Schmidt, Martin; Streblow, Rita; Müller, Dirk; Kosmatopoulos, Elias. "A multifunctional demonstration bench for advanced control research in buildings : monitoring, control, and interface system". IEEE IECON 2013 proceedings : 39th Annual Conference of the IEEE Industrial Electronics Society ; Vienna, Austria.

9.5 Short CV of scientists involved in the project

Dipl.-Wirt.-Ing. Johannes Peter Fütterer

- 2004 - 2010: Diploma, Industrial Engineering, RWTH Aachen University
- 2008 - 2009: Abroad studies, École Polytechnique Fédérale de Lausanne, EPFL, Switzerland
- Since 08.2010: Research Associate, Institute for Energy Efficient Buildings and Indoor Climate, E.ON ERC, RWTH Aachen University

Dipl.-Wirt.-Ing. Ana Constantin

- 2010: Diploma, Industrial Engineering and Business Administration, RWTH Aachen University
- Since 09.2010: Research Associate, Institute for Energy Efficient Buildings and Indoor Climate, E.ON ERC, RWTH Aachen University

Prof. Dr.-Ing. Dirk Müller
Education:

- 1989-1995: Diploma, Mechanical Engineering, RWTH Aachen University
- 1993-1994: DAAD Scholarship: Bachelor of Engineering, Dartmouth College, USA
- 1995-2000: Scientific Researcher, Lehrstuhl für Wärmeübertragung und Klimatechnik, RWTH Aachen University, Doctoral Degree
- 1998-2000: Business Studies, Fernuniversität Hagen, Certificate

Academic Visits:

- 1999-2002: Robert Bosch GmbH, Research and Advanced Engineering, Project Leader
- 2002-2003: Behr GmbH & Co., Advanced Simulation Tools and Processes, Manager
- 2003-2007: Professor at the Technical University of Berlin, Head of the Hermann-Rietschel-Institute
- Since 2007: Professor at the RWTH Aachen University, Head of the Institute for Energy Efficient Buildings and Indoor Climate

Additional Business:

- Since 2007: Supervisory Board Member and Engineering Consultant, TROX GmbH

Professional Recognitions, Awards and Honours:

- 2000: Borchers-Plakette, RWTH Aachen University
- 2002: Award for Young Reseachers, German Society of Refrigeration and Air Conditioning
- 2004: Ring of Honour, Association of German Engineers
- Since 2006: Board Member, German Society of Refrigeration and Air Conditioning
- Since 2008: Chairman, Expert Commission, Fachinstitut Gebäude-Klima e.V.

9.6 Project timeline

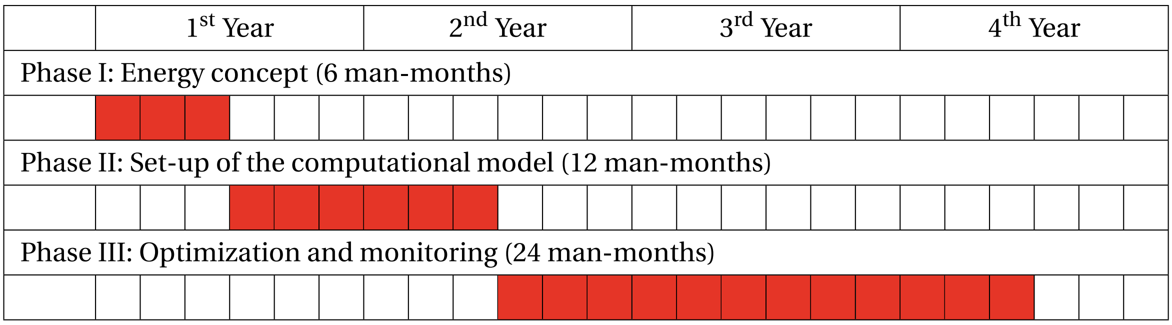

Project synopsis

Johannes Peter Fütterer, Ana Constantin, Dirk Mueller

EBC - Institute for Energy Efficient Buildings an Indoor Climate
E.ON Energy Research Center (E.ON ERC), RWTH Aachen University
Mathieustr. 10
52074 Aachen, Germany

Dipl.-Wirt.-Ing.	Dipl.-Wirt.-Ing.	Univ.-Prof. Dr.-Ing.
Johannes Peter Fütterer	Ana Constantin	Dirk Mueller
Tel.: +49 241/80 49790	Tel.: +49 241/80 49793	Tel.: +49 241/80 49761
Fax.: +49 241/80 49769	Fax: +49 241/80 49769	Fax: +49 241/80 49769
jfuetterer@eonerc.rwth-aachen.de	aconstantin@eonerc.rwth-aachen.de	dmueller@eonerc.rwth-aachen.de

Categories E.ON ERC focus

☐	Small Scale CHP	☐	Large Power Plants
☐	Energy Storage	☑	Energy Efficiency
☐	Consumer Behavior	☐	Energy Economics Modeling
☑	Energy and Buildings	☐	Power Electronics
☐	Distribution Networks	☑	Renewable Energy
☐	Carbon Storage (CCS)	☐	Others: Medium-Size Power Plants

Type of project report:	Final Project Report
Start and end date of project:	01 2008 - 06 2012
Start and end of project pause:	07 2009 - 06 2010
Project in planned timelines:	☑ yes ☐ no

Participating Chairs of E.ON ERC

☐	Automation of Complex Power Systems (ACS)
☑	Energy Efficient Buildings and Indoor Climate (EBC)
☐	Future Energy Consumer Needs and Behavior (FCN)
☐	Applied Geophysics and Geothermal Energy (GGE)
☐	Power Generation and Storage Systems (PGS)

Acknowledgments

This project was supported by a grant of E.ON ERC gGmbH.

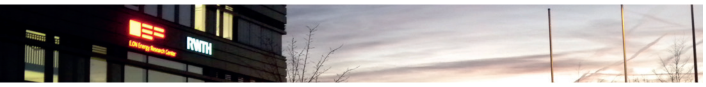

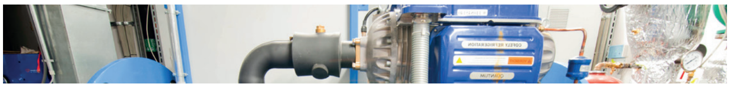

E.ON Energy Research Center Series

ISSN: 1868-7415
First Edition: Aachen, Juni 2012

E.ON Energy Research Center,
RWTH Aachen University

Mathieustraße 10
52074 Aachen
Germany

T +49 (0)241 80 49667
F +49 (0)241 80 49669
post_erc@eonerc.rwth-aachen.de
www.eonerc.rwth-aachen.de